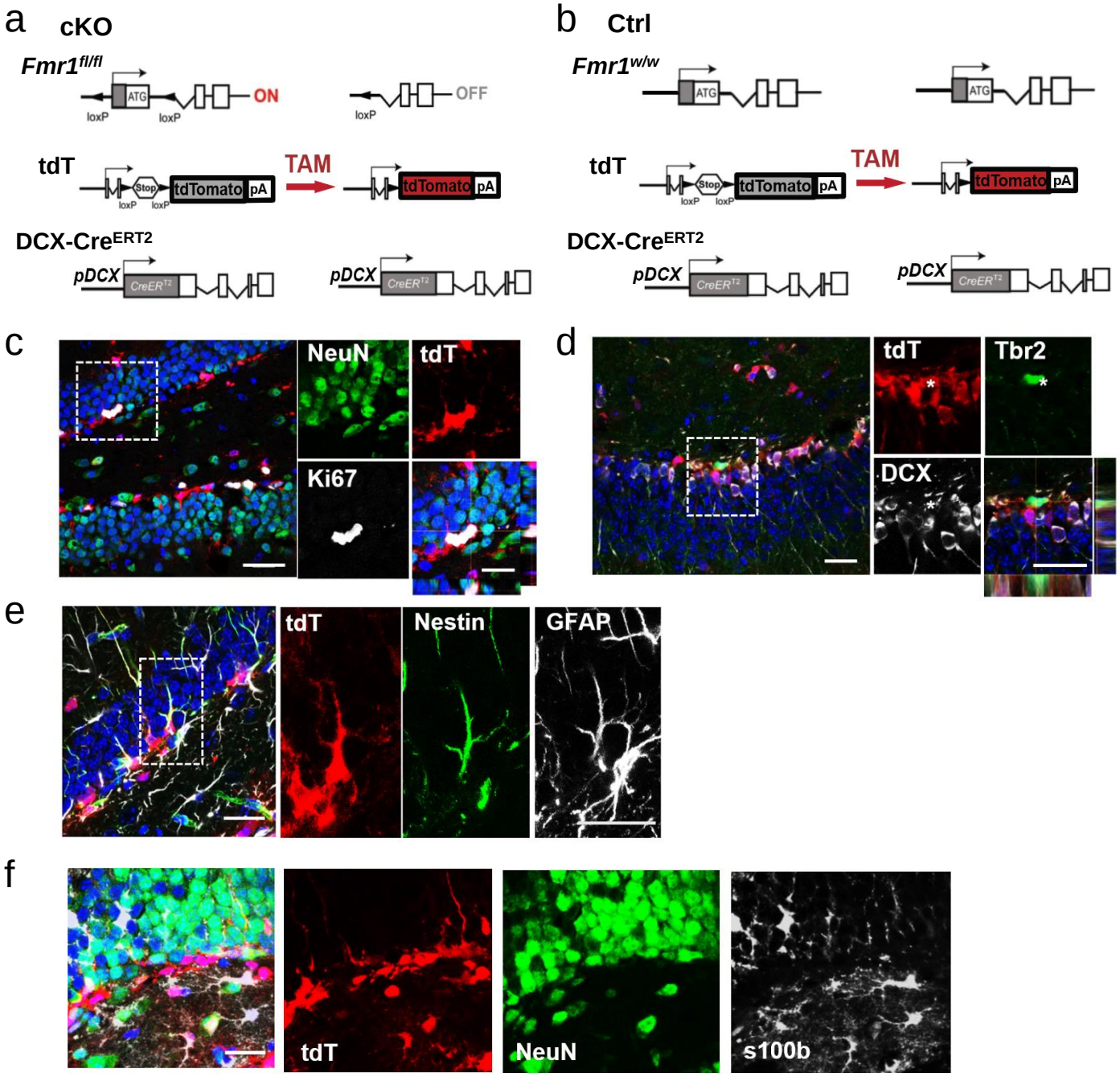

Supplementary Figure 1: Generation of inducible immature neuron-specific *Fmr1* knock out mice.

a, Administration of tamoxifen to adult cKO mice results in the removal of the first exon of the mouse *Fmr1* gene and the "Stop" signal of tdTomato in DCX-expressing immature neurons. This abolishes the expression of FMRP but ensures the expression of tdTomato (tdT) in DCX-expressing neurons. **b,** Administration of tamoxifen to adult cKO mice results in the expression of tdTomato in DCX-expressing neurons. **c-f,** Sample confocal images (from 3 independently repeated experiments with similar results) of neuronal markers staining of brain sections from Ctrl;Cre;tdT mice on Day 3 post TAM injection: **c,** NeuN (green for mature neurons), Ki67 (white for dividing cells) and tdT (Red for Cre-reporter); **d,** Tbr2 (green for neuroblasts), DCX (white for immature neurons) and tdT (Red); **e,** Nestin(green for neural stem and progenitor cells), GFAP (white for radial glia like cells and astrocytes) and tdT (Red); **f,** NeuN (green), s100β (white for astrocytes) and tdT (Red).. Scale bars, 50 μm.

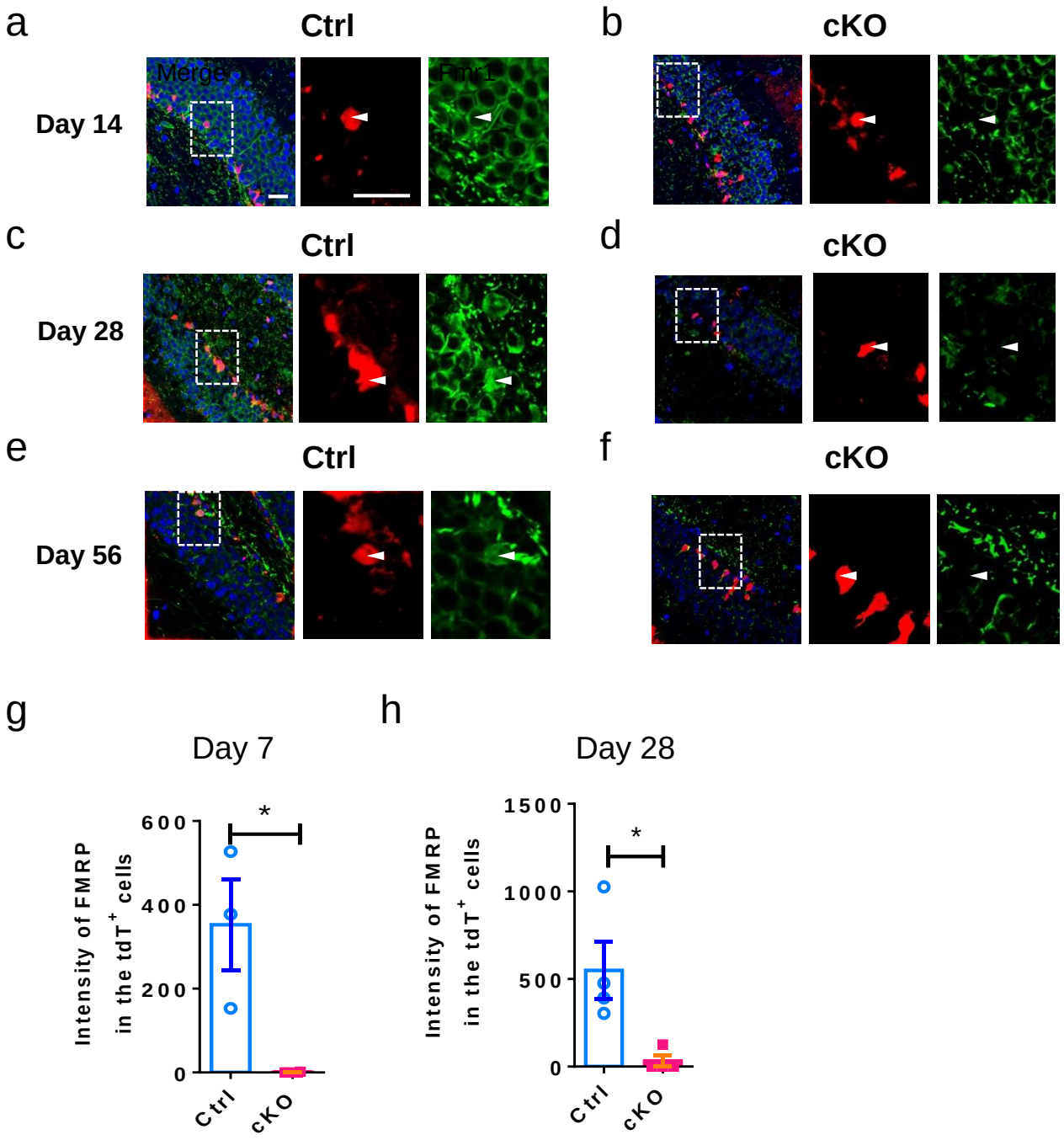

Supplementary Figure 2: FMRP is deleted in tdT+ neurons in the cKO mice

a-f, Sample confocal images (from 3 independently repeated experiments with similar results) of FMRP (green) staining of brain sections from Ctrl;Cre;tdT and cKO;Cre;tdT mice at Day 14, Day 28, Day 56 after tamoxifen injection.. Scale bars, 20 μm. **g,** The expression level of FMRP in the tdT+ cells of the DG from cKO; Cre; tdTomato mice at Day 7 after tamoxifen injection (Student's t-test, two-sided. $t(5) = 3.870$, $^*P = 0.0118$. Ctrl: 352.5 ± 108.7, n = 3 mice; cKO: 0.5424 ± 0.5424, n = 4 mice). **h,** The expression level of FMRP in the tdT+ cells of the DG from cKO; Cre; tdTomato mice at Day 28 after tamoxifen injection (Student's t-test, two-sided. $t(6) = 3.127$, $^*P = 0.0204$. Ctrl: 549.5 ± 162.6, n = 4 mice; cKO: 31.47 ± 31.47, n = 4 mice). *P < 0.05. All error bars reflect the Mean ± S.E.M.

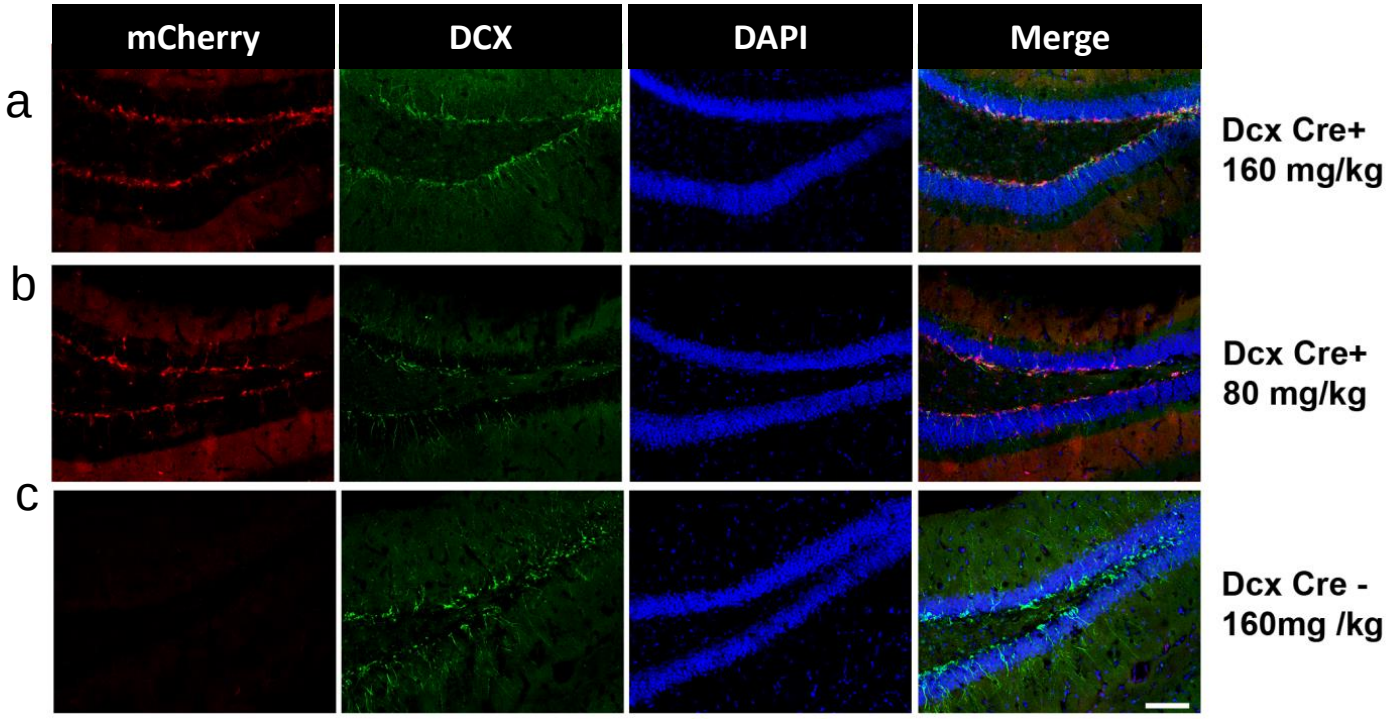

Supplementary Figure 3: Recombination in tdT mice requires the presence of Cre recombinase a, Sample confocal images (from 3 independently repeated experiments with similar results) of DG of Ctrl;Cre;tdT mice after TAM (160 mg/kg, i.p.) injection. b, Images of DG of Ctrl;Cre;tdT mice after TAM (80 mg/kg, i.p.) injection. c, Images of DG of Ctrl;Cre-;tdT (no Cre) mice after TAM (160 mg/kg, i.p.) injection.. Scale bars, 20 μm

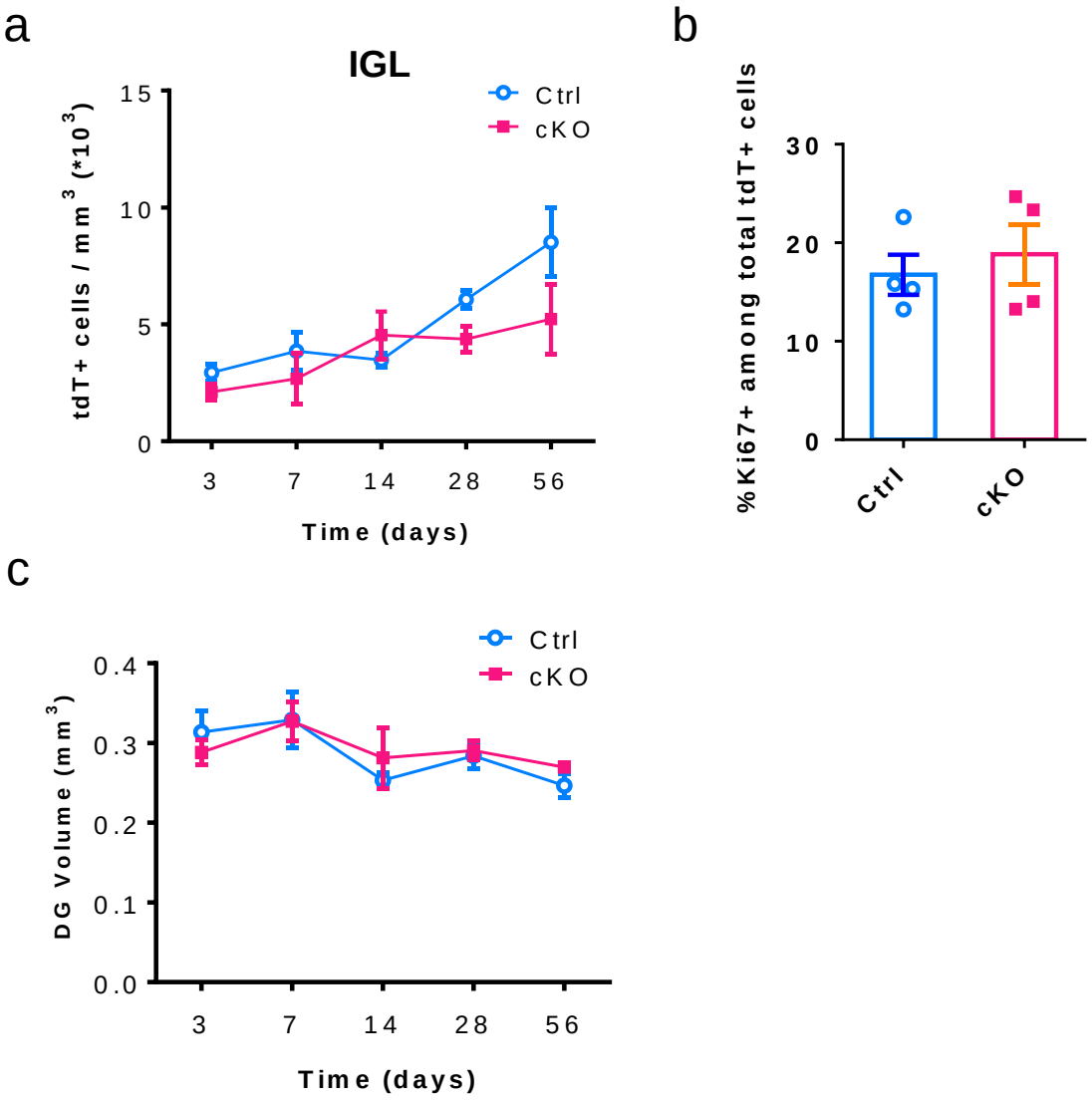

Supplementary Figure 4: Deletion of FMRP in DCX+ developing neurons did not affect proliferation and DG volume.

a, Quantitative comparison of tdT+ neuronal numbers in the IGL of cKO;Cre;tdT mice and Ctrl;Cre;tdT mice (two-way ANOVA with Bonferroni post hoc test: F (4, 39) = 1.682, *P* = 0.1738. Day 3: Ctrl, 2.939 ± 0.3555, n = 5 mice; cKO, 2.107 ± 0.3449, n = 5 mice. Day 7: Ctrl, 3.851 ± 0.8111, n = 5 mice; cKO, 2.681 ± 1.100, n = 4 mice. Day 14: Ctrl, 3.478 ± 0.3118, n = 5 mice; cKO, 4.539 ± 1.013, n = 5 mice. Day 28: Ctrl, 6.065 ± 0.3894, n = 6 mice; cKO, 4.368 ± 0.5556, n = 5 mice. Day 56: Ctrl,, 6.065 ± 0.3894, n = 5 mice; cKO, 5.228 ± 1.490, n = 4 mice). **b,** Percentage of Ki67+ in total tdT+ cells in SGZ of cKO;Cre;tdT mice and Ctrl;Cre;tdT mice at Day 3 after tamoxifen injection (Student's t-test, two-sided. t(6) = 0.5717, *P* = 0.5883. Ctrl, 16.75 ± 2.030, n = 4 mice; cKO, 18.83 ± 3.010, n = 4 mice). **c,** Quantitative comparison of DG volume of cKO;Cre;tdT mice and Ctrl;Cre;tdT mice. (two-way ANOVA with Bonferroni post hoc test: F (4, 35) = 0.4430, *P* = 0.7767. Day 3: Ctrl, 0.3135 ± 0.02695, n = 5 mice; cKO, 0.2882 ± 0.01517, n = 4 mice. Day 7: Ctrl, 0.3290 ± 0.03451, n = 5 mice; cKO, 0.3271 ± 0.02486, n = 4 mice. Day 14: Ctrl, 0.3290 ± 0.03451, n = 5 mice; cKO, 0.3271 ± 0.02486, n = 4 mice. Day 28: Ctrl, 0.2837 ± 0.01567, n = 5 mice; cKO, 0.2906 ± 0.01176, n = 4 mice. Day 56: Ctrl,, 0.2467 ± 0.01470, n = 5 mice; cKO, 0.2697 ± 0.007089, n = 4 mice). All error bars reflect the Mean ± S.E.M.

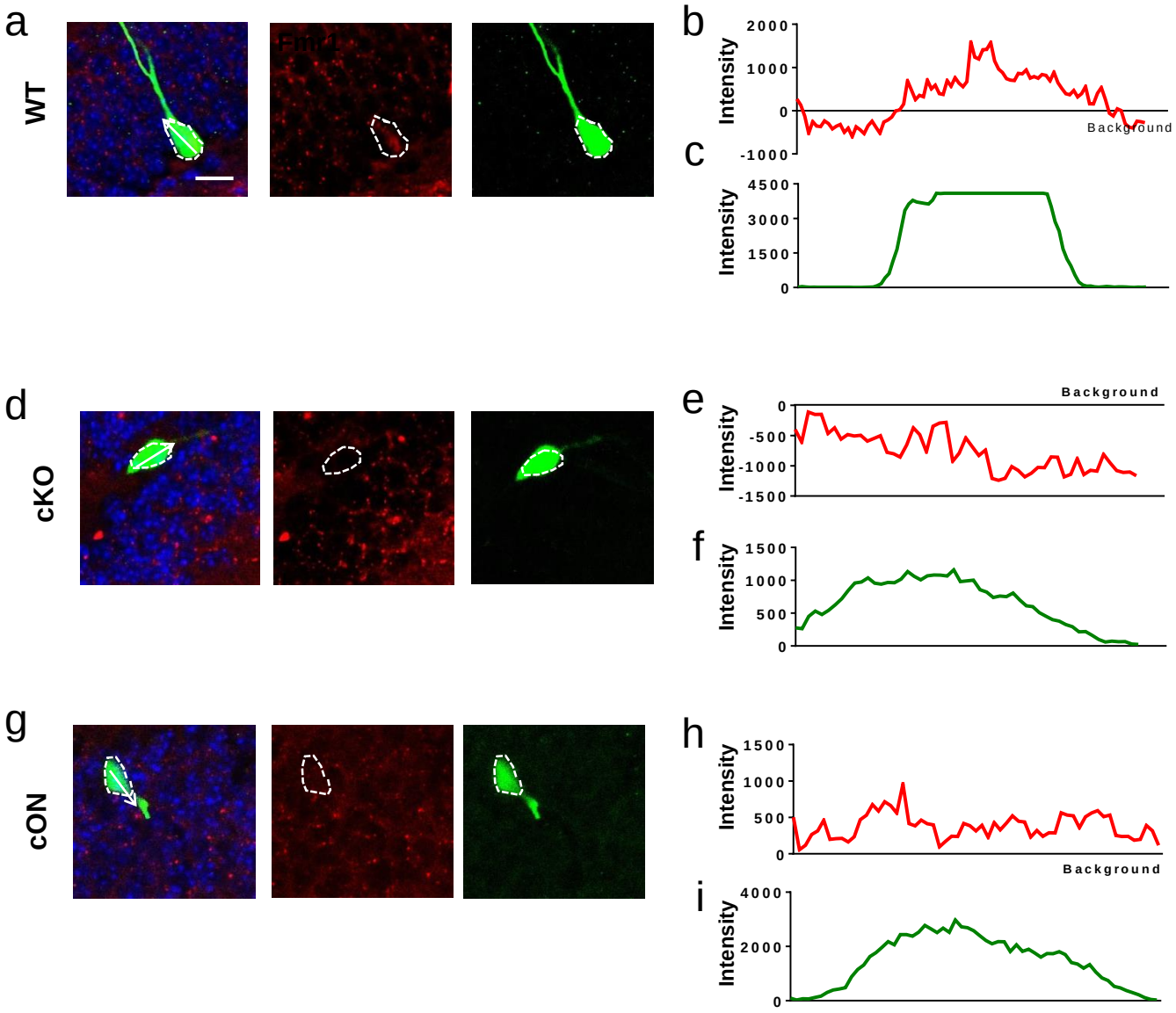

Supplementary Figure 5. Deletion or restoration of FMRP in DCX+ immature neurons in DG using Retrovirus-pDcx-Cre.

a, d, g, Sample confocal images (from 3 independently repeated experiments with similar results) of DG of WT, *Fmr1*-cKO, and *Fmr1*-cON mice injected with Retrovirus-*pDcx*-Cre and Retrovirus-Flip-GFP. Scale bars, 20um. Intensity of FMRP and GFP signal was measured along the yellow line. b-c, e-f, h-i, Intensity measurements for FMRP (red-line) and GFP (green-line) in WT mouse (b,c), *Fmr1*-cKO mouse (e,f) and *Fmr1*-cON mouse (h,i) injected with retrovirus.

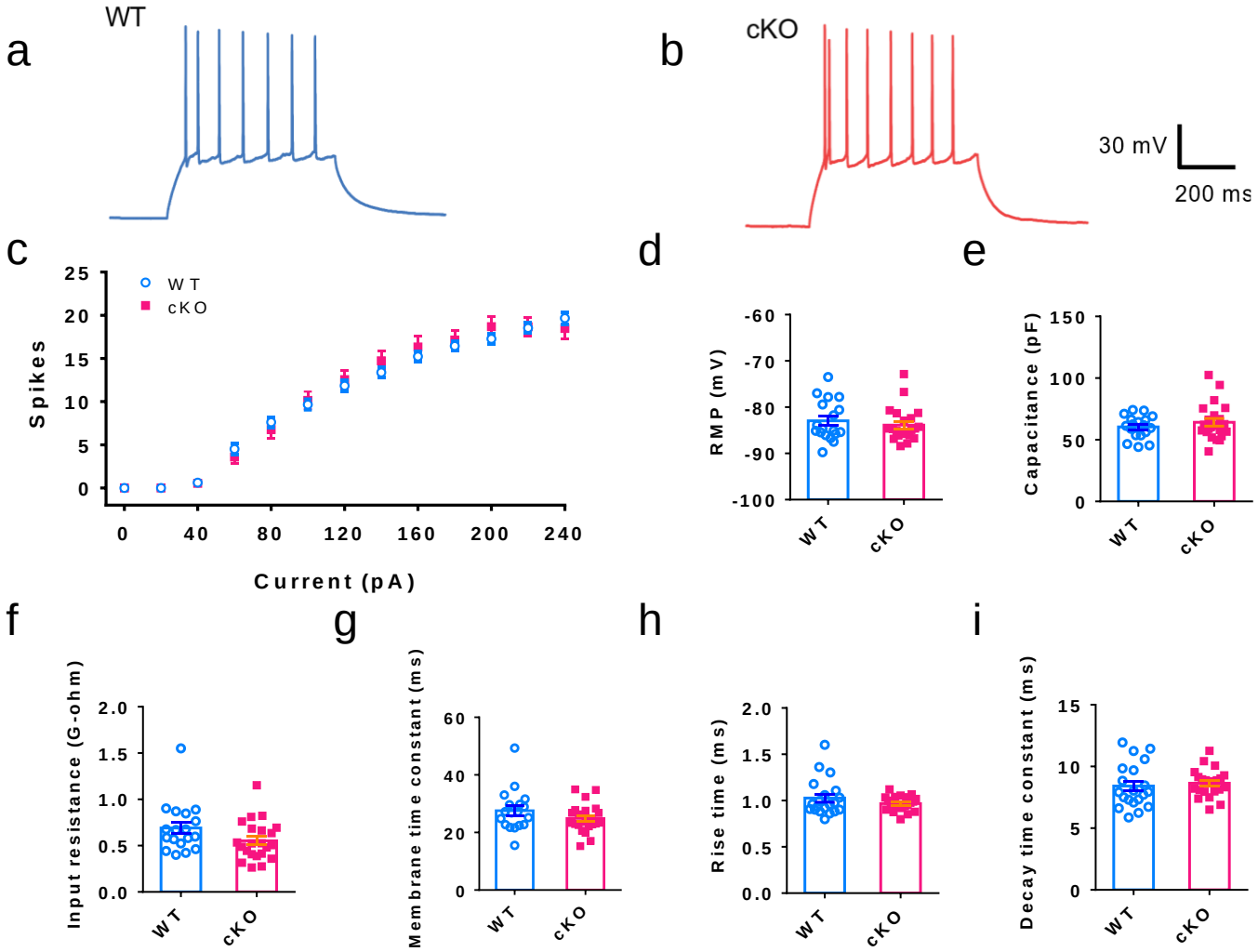

Supplementary Figure 6: FMRP-deficient DCX+ immature neurons in the adult DG exhibited no significant deficits in intrinsic physiological properties.

a, b, Example of AP (action potential) trains (from independent experiments on 6 WT mice and 8 cKO mice with similar results) upon current injections recorded from GFP+ neurons in the DG slices from WT and cKO. **c-g,** intrinsic properties of GFP+ neurons in the DG slices from WT and cKO: **c,** Action potential spikes upon current injections (Multi-ANOVA, $F(1,39) < 0.001$, $P = 0.991$. Current = 40 pA: WT, 0.6111 ± 0.3040 n =18; cKO, 0.5455 ± 0.2691 n =22. Current = 60 pA: WT, 4.500 ± 0.6170 n =18; cKO,3.591 ± 0.8076 n =22. Current = 80 pA: WT, 7.611 ± 0.5667 n =18; cKO, 6.773 ± 1.008 n =22.Current = 100 pA: WT, 9.667 ± 0.6468 n =18; cKO,10.14 ± 1.024 n =22. Current = 120 pA: WT, 11.83 ± 0.6223 n =18; cKO, 12.55 ± 1.108 n =22. Current = 140 pA: WT, 13.39 ± 0.5893 n =18; cKO, 14.73 ± 1.163 n =22. Current = 160 pA: WT, 15.22 ± 0.5805 n =18; cKO, 16.33 ± 1.293 n =21. Current = 180 pA: WT, 16.44 ± 0.5475 n =16; cKO, 17.15 ± 1.057 n =20. Current = 200 pA: WT, 17.27 ± 0.5893 n =15; cKO, 18.68 ± 1.175 n =19. Current = 220 pA: WT, 18.53 ± 0.5925 n =15; cKO, 18.67 ± 1.042 n =18. Current = 240 pA: WT, 19.67 ± 0.7213 n =12; cKO,18.47 ± 1.171 n =15. 18 cells from 6 WT mice and 22 cells from 8 cKO mice). **d,** Resting membrane potential (Student's t-test, two-sided. $t(38) = 0.7389$, $P = 0.4645$. WT, -82.95 ± 1.026, n = 18. cKO, -83.88 ± 0.7747, n = 22). **e,** Capacitance (Student's t-test, two-sided. $t(38) = 0.9283$, $P = 0.3591$. WT, 60.48 ± 2.167, n = 18. cKO, 64.17 ± 3.129, n = 22). **f,** Input resistance (Student's t-test, two-sided. $t(38) = 1.819$, $P = 0.0767$. WT, 0.6908 ± 0.06344, n = 18. cKO, 0.5524 ± 0.04525, n = 22). **g,** Membrane time constant (Student's t-test, two-sided $t(38) = 1.401$, $P = 0.1694$. WT, 27.58 ± 1.719, n = 18. cKO, 24.85 ± 1.061, n = 22). **h,** Average rise time of mEPSCs (Student's t-test, two-sided $t(40) = 1.300$, $P = 0.2012$. WT, 1.027 ± 0.04447, n = 18. cKO, 0.9672 ± 0.01662, n = 22). **i,** Average decay time constant of mEPSCs (Student's t-test, two-sided $t(40) = 0.4749$, $P = 0.6374$. WT, 8.420 ± 0.4030, n = 18. cKO, 8.638 ± 0.2385, n = 22). All error bars reflect the Mean ± S.E.M.

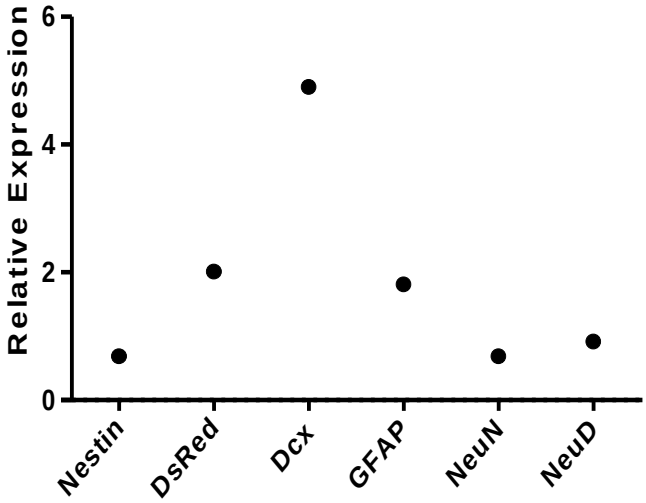

Supplementary Figure 7: Validation of relative enrichment of genes in FACS isolated immature neurons using real time PCR

Relative enrichment of each gene was determined by real time PCR, with equal numbers of sorted cells used to generate cDNA. Cells from the DsRed+ gate show a pronounced enrichment of immature neuron markers (*Dcx*) and low enrichment of stem cell markers (*Nestin)*, radial glia and astrocyte marker (*Gfap*), mature neuronal marker (*NeuN*), and control DsRed (n = 1 with >3 experimental triplicates for PCR).

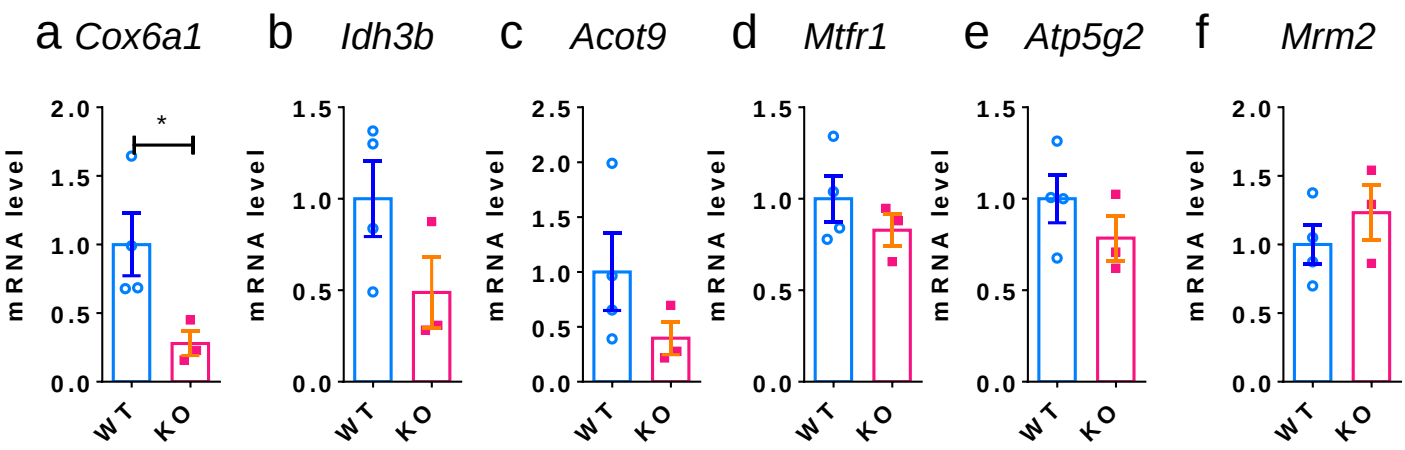

Supplementary Figure 8. Quantification analyses of mRNA levels of DE genes involved in regulation of mitochondrial functions in WT and Fmr1 KO primary hippocampal neurons at DIV 7. **a-f,** Quantification analyses of mRNA levels of DE genes related to mitochondrial metabolism in WT and Fmr1KO primary hippocampal cells. *Gapdh* was used as the internal control for quantitative PCR analysis. (Student's t-test, two-sided. *Cox6a1*, WT = 1.000 ± 0.2271, n = 4 mice; KO = 0.2791 ± 0.08782, n = 3 mice. t(5) = 2.588, *P* = 0.0490; *Idh3b*, WT = 1.000 ± 0.2067, n = 4 mice; KO = 0.4885 ± 0.1934, n = 3 mice. t(5) = 1.744, *P =0.1416*; *Acot9*, WT = 1.000 ± 0.3503, n = 4 mice; KO = 0.3974 ± 0.1504, n = 3 mice. t(5) = 1.391, *P* = 0.2229; *Mtfr1*, WT = 1.000 ± 0.1265, n = 4 mice; KO = 1.000 ± 0.1265, n = 3 mice. t(5) = 0.3506, *P* = 0.3506; *Atp5g2*, WT = 1.000 ± 0.1307, n = 4 mice; KO = 0.7850 ± 0.1229, n = 3 mice. t(5) = 1.158, *P* = 0.2991; *Mrm2*, WT = 1.000 ± 0.1446, n = 4 mice; KO = 1.233 ± 0.1981, n = 3 mice. t(5) = 0.9767, *P* = 0.3736). *P < 0.05. All error bars reflect the Mean ± S.E.M.

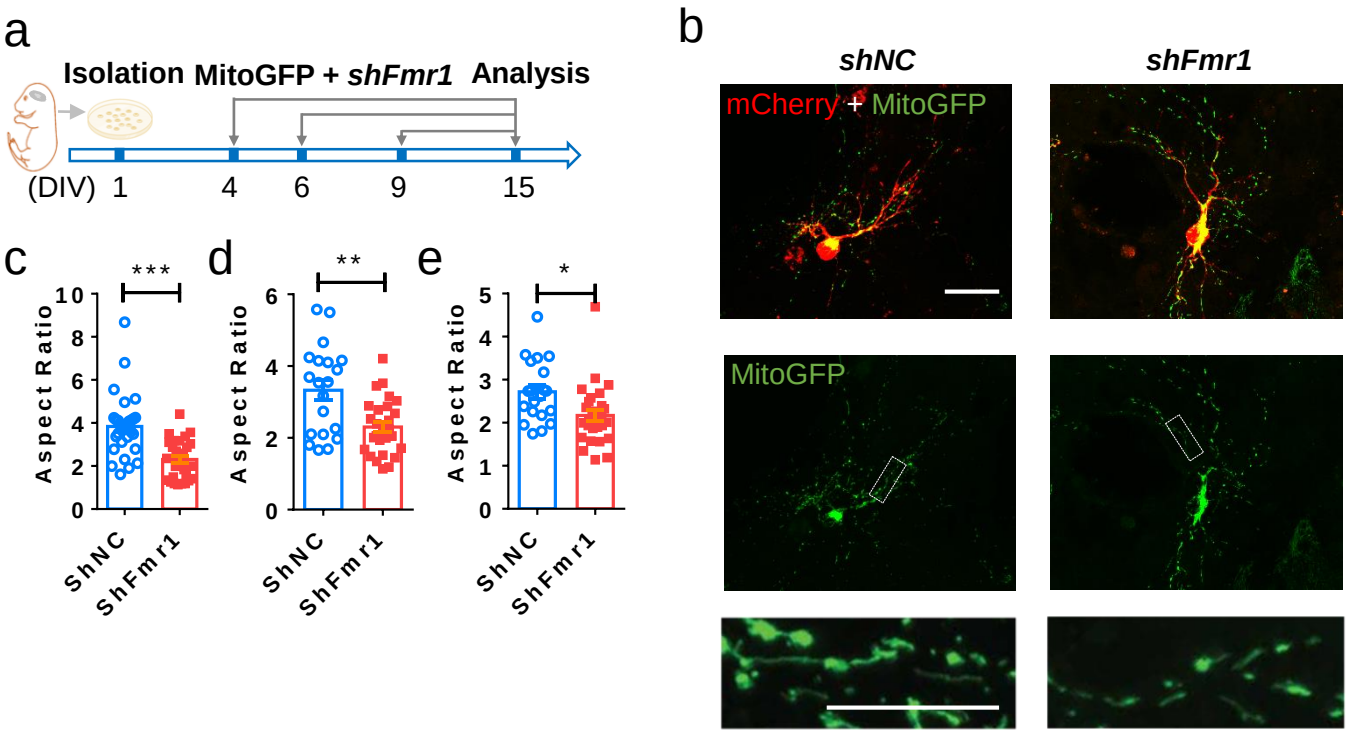

Supplementary Figure 9: Impaired mitochondrial aspect ratio in FMR1-deficient DCX+ immature neurons.

a, Experimental scheme for assessing the mitochondrial morphology in DIV15 primary hippocampal neurons transfected with MitoGFP and *shFmr1*-mCherry or shNC-mCherry at DIV 4, 6 or 9. **b,** Sample confocal images (from 3 independently repeated experiments with similar results) of mitochondria in the DIV 15 primary hippocampal neurons transfected with MitoGFP and *shFmr1* or shNC at DIV 4Scale bar, 10 µm. **c-e,** Quantitative comparison of mitochondrial aspect ratio of DIV15 primary hippocampal neurons transfected with *shFmr1* or shNC at DIV 4 (**c,** Student's t-test, two-sided. t(54) = 4.661, *P* < *0.0001*. *shNC*: 3.841 ± 0.2710 n=29 cells; *shFmr1*: 2.302 ± 0.1799 n=27 cells from 3 biologically independent neuronal isolations), at DIV 6 (**d,** Student's t-test, two-sided. t(45) = 3.493, *P* = 0.0011. *shNC*: 3.328 ± 0.2765 n=20 cells; *shFmr1*: 2.302 ± 0.1489 n=27 cells from 3 biologically independent neuronal isolations), at DIV 9 (**e,** Student's t-test, two-sided. t(45) = 2.619, *P* = 0.012. *shNC*: 2.718 ± 0.1590 n=20 cells; *shFmr1*: 2.170 ± 0.1359 n=27 cells from 3 biologically independent neuronal isolations). *P < 0.05, **P < 0.01, ***P < 0.001. All error bars reflect the Mean ± S.E.M.

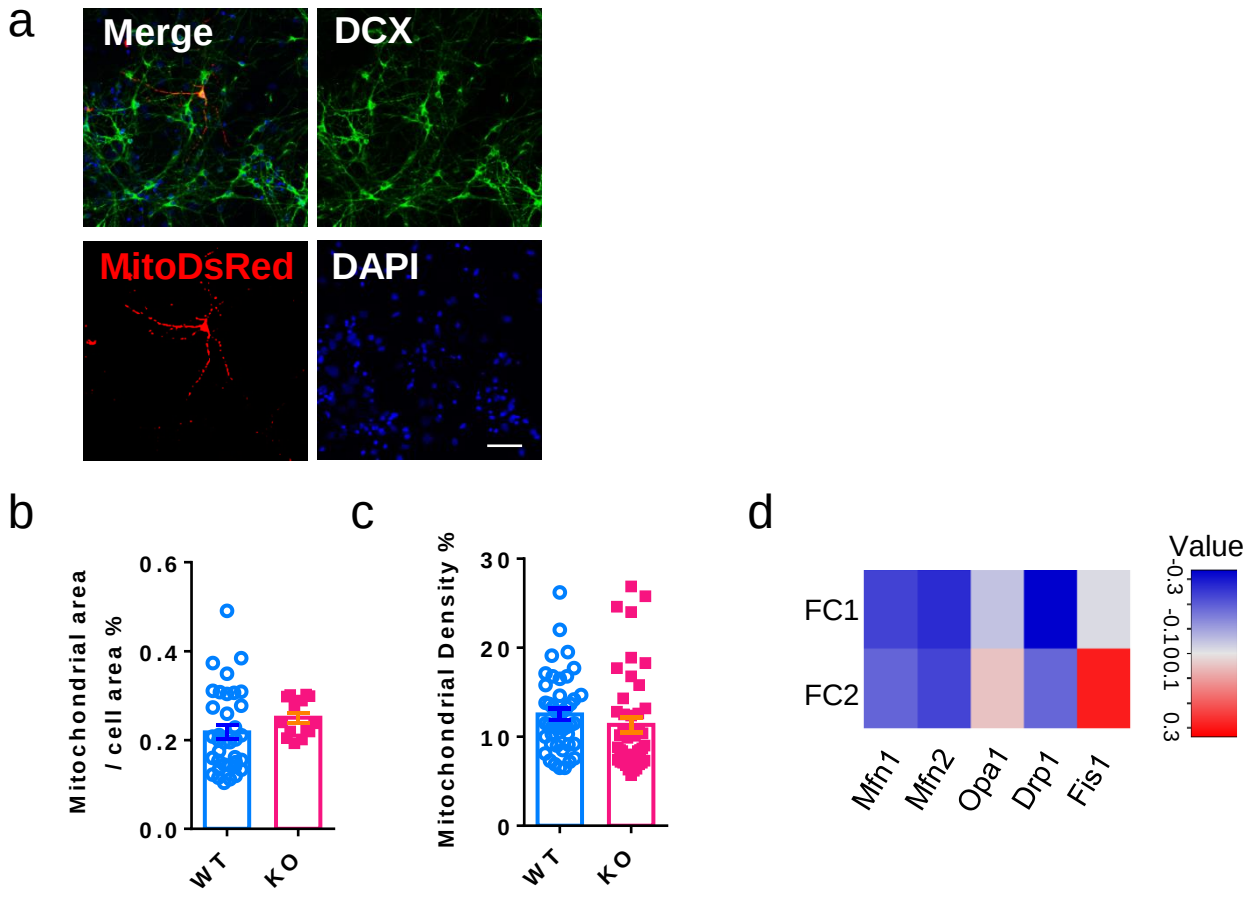

Supplementary Figure 10. FMRP deficiency does not affect mitochondrial area or density in developing neurons.

a, Sample confocal images (from 3 independently repeated experiments with similar results) of DIV 7 primary hippocampal neurons transfected with MitoDsRed. DCX (green), MitoDsRed (red), DAPI (blue). Scale bars, 50 μm. All (100%) MitoDsRed+ neurons expressed DCX.. **b,** Mitochondrial density in the proximal dendrites (Student's t-test, two-sided. t(88) = 1.114, *P* = 0.2685. WT, 0.2171 ± 0.01543, n =36; cKO, 0.2504 ± 0.01119 n =14 cells from 3 different animals). **c,** Mitochondrial area (Student's t-test, two-sided. t(48) = 1.289, *P* = 0.2035. WT, 12.51 ± 0.6346, n =45; cKO, 11.35 ± 0.8310 n =45 cells from 3 different animals). **d,** Heatmap of the expression of mitochondrial fusion and fission genes among 519 differentially expressed genes in *Fmr1* KO DsRed+ immature neurons obtained by FACS-seq (Figure 3). All error bars reflect the Mean ± S.E.M.

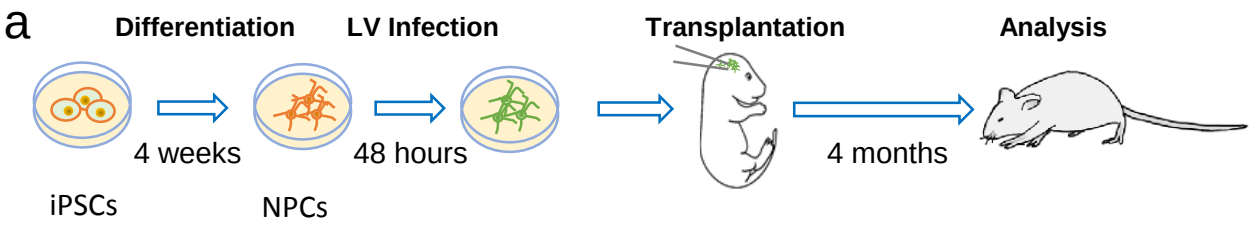

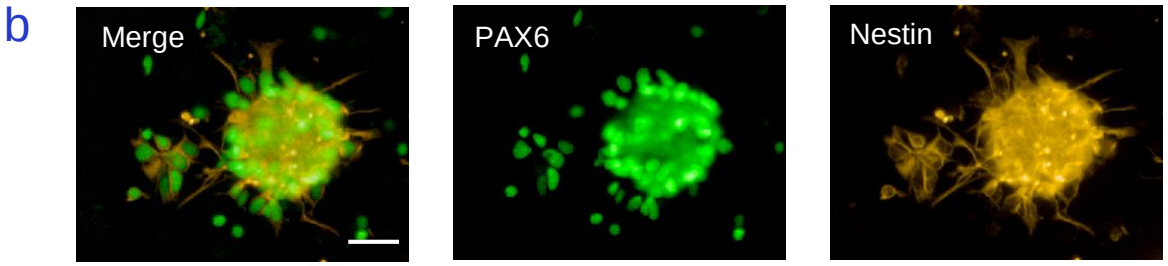

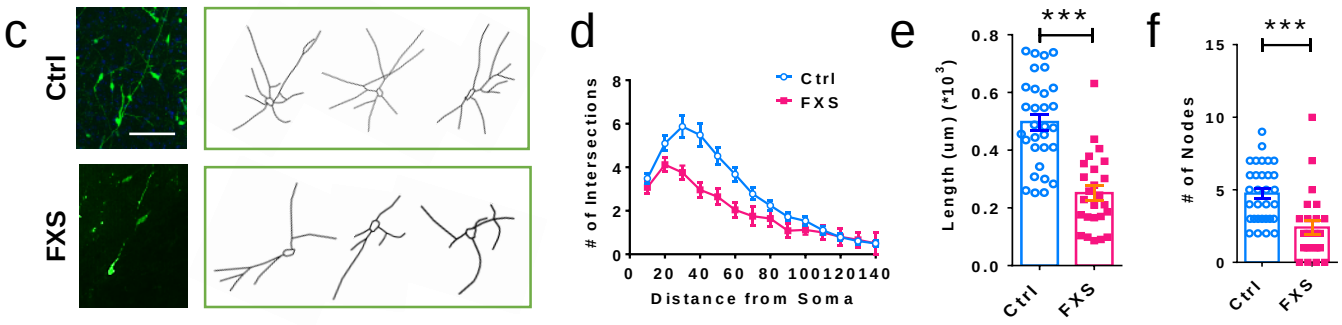

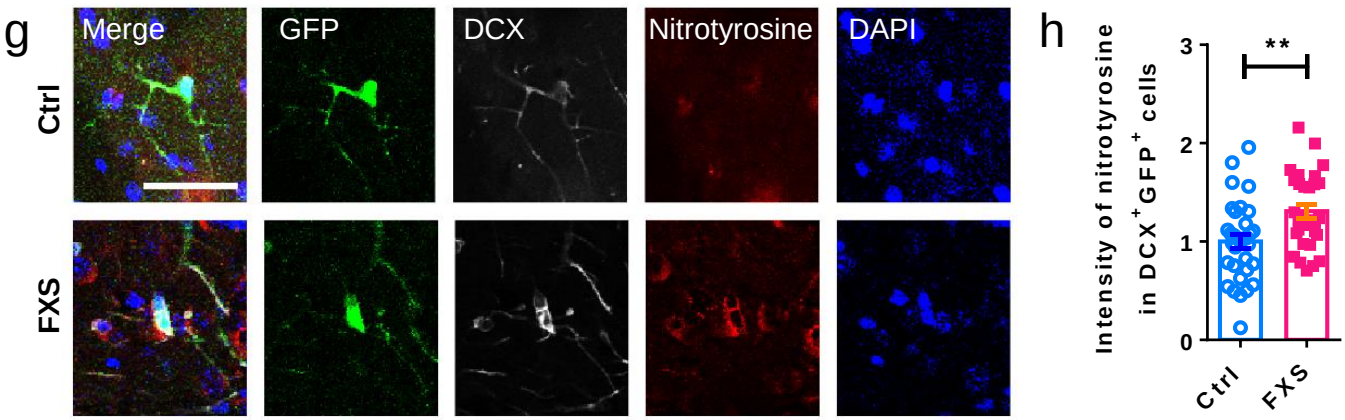

Supplementary Figure 11: Human FXS neurons developed in transplanted mouse brains exhibit impaired maturation and **increased oxidative stress.**
(see figure legend on the next page)

Supplementary Figure 11: Human FXS neurons developed in transplanted mouse brains exhibit impaired maturation and **increased oxidative stress**

a, Experimental scheme for transplanting neuroprogenitors (NPCs) differentiated from FXS patient-derived induced pluripotent stem cells (iPSCs) and assessing dendritic maturation of human FXS neurons in transplanted immunodeficient mouse cortex**. b,** Representative images of NPCs (from 3 independently repeated experiments with similar results) for transplantation. Sample confocal images showing PAX6 and Nestin double positive cells.. Scale bar, 50 µm. **c,** Examples of confocal images (from 3 independently repeated experiments with similar results) and Neurolucida software-created traces of GFP+ FXS and Control neurons. **d-f,** Dendritic complexity analysis of GFP+ transplanted neurons. **d,** Scholl analysis (Multi-ANOVA, $F_{1,56}$= 50.021, $P < 0.0001$. Ctrl: n= 31 cells from 3 mice; FXS: n=25 cells from 3 mice); **e,** dendritic length (Student's t-test, two-sided. $t(54) = 6.331$, $P < 0.0001$. Ctrl = 0.4975 ± 0.02777, n = 31; FXS = 0.2515 ± 0.02618, n = 25 cells from 3 mice). **f,** Dendritic nodes (Student's t-test, two-sided. $t(54) = 4.099$, $P < 0.0001$. Ctrl = 4.742 ± 0.3531, n = 31; FXS = 2.400 ± 0.4619, n = 25 cells from 3 mice). **g,** Sample confocal images (from 3 independently repeated experiments with similar results) of nitrotyrosine (red), DCX (far red) staining of brain sections from SCID mice 4 months post-transplantation.. Scale bars, 50 µm. **h,** The expression level of nitrotyrosine in the DCX+GFP+ cells in mouse cortex (Student's t-test, two-sided. $t(61) = 3.138$, $P = 0.026$. Ctrl = 1.000 ± 0.06967, n = 33; FXS = 1.309 ± 0.06942, n = 30 cells from 3 mice). **P < 0.01, ***P < 0.001. All error bars reflect the Mean ± S.E.M.

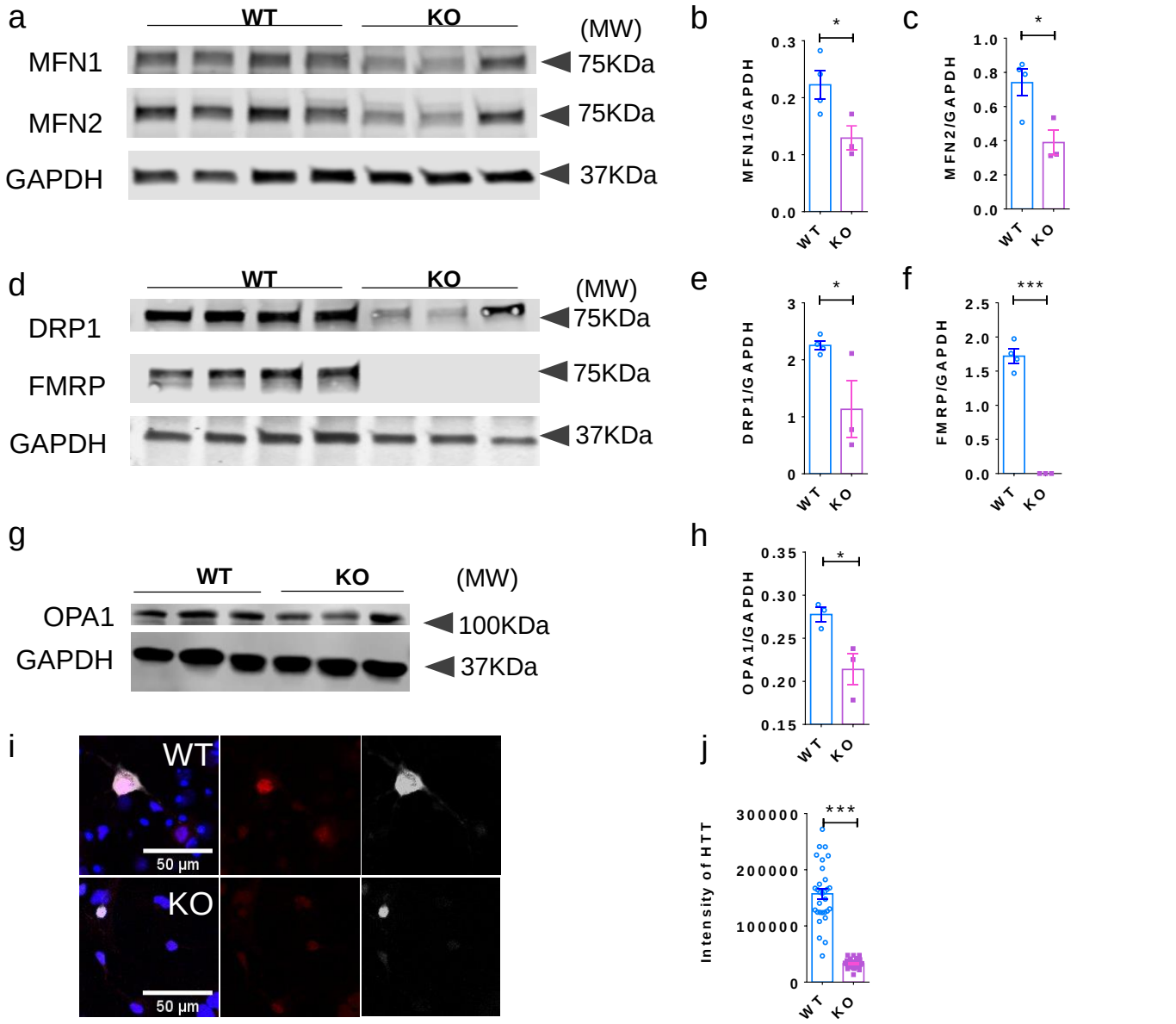

Supplementary Figure 12. Mitochondrial fusion and fission Protein levels in *Fmr1* KO primary hippocampal neurons.

a-h, Western blot analyses of mitochondrial fusion and fission proteins in WT and *Fmr1* KO primary cells. **a-c,** Representative cropped western blot images (see Supplementary Figure 23 for full images of western blots) **(a**) and quantitative analysis of MFN1 (**b,** Student's t-test, two-sided. t(5) = 2.726, *P=0.0415*. WT: 0.2227 ± 0.02472, n=4; KO: 0.1292 ± 0.02137, n=3 biologically independent isolations) and MFN2 (**c,** Student's t-test, two-sided. t(5) = 3.168, *P=0.0249.* WT: 0.7401 ± 0.07829, n=4; KO: 0.3892 ± 0.07255, n=3 biologically independent isolations). **d-f,** Western blot image **(d**) and quantitative analysis of DRP1 (**e,** Student's t-test, two-sided. t(5) = 2.643, *P=0.0458.* WT: 2.254 ± 0.07586, n=4; KO: 1.132 ± 0.4958, n=3 biologically independent isolations) and FMRP (**f,** Student's t-test, two-sided. t(5) = 13.95, *P<0.0001.* WT: 1.719 ± 0.1041, n=4; KO: 0.0 ± 0.0, n=3 biologically independent isolations). **g-h,** Representative cropped western blot images (see Supplementary Figure 23 for full images of western blots). **(g**) and quantitative analysis of OPA1 (**h,** Student's t-test, two-sided. t(4) = 3.181, *P= 0.0335.* WT: 0.2776 ± 0.008473, n=4; KO: 0.2138 ± 0.01818, n=3 biologically independent isolations) . **i-j,** Signal intensity measurement of HTT in WT and *Fmr1* KO primary cells. **i,** Representative images (from 3 independently repeated experiments with similar results) of cells stained with dapi (blue), anti-HTT (red), and anti-Neun (grey).. **j, Q**uantitative analysis of Htt intensity (Student's t-test, two-sided. t(58) = 12.75, *P < 0.0001.* WT: 157088 ± 9643, n=30; KO: 32753 ± 1474, n=30 cells from 3 biologically independent isolations*)*. *P < 0.05, ***P < 0.001. All error bars reflect the Mean ± S.E.M.

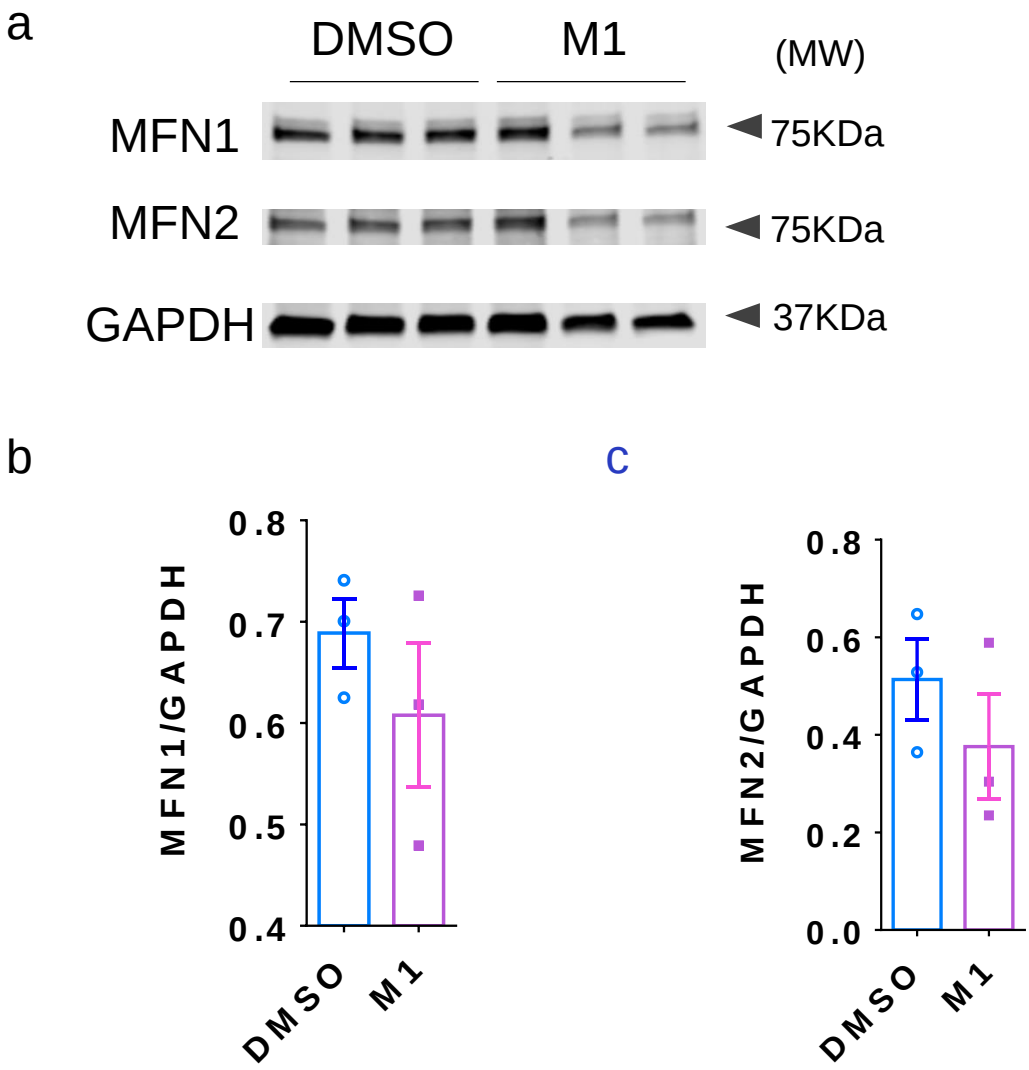

Supplementary Figure 13. MFN1 and MFN2 protein levels in neurons are not affected by M1 treatment

(a) Representative cropped western blot images (see Supplementary Figure 24 for full images of western blots) of mitofusin proteins in WT primary neurons treated with M1 or DMSO. (b, c) quantitative analysis of MFN1 (**b,** Student's t-test, two-sided. t(4) = 1.027, *P=0.3626.* DMSO: 0.6889 ± 0.03393, n=3; M1: 0.6078 ± 0.07134, n=3 biologically independent isolations) and MFN2 (**c,** Student's t-test, two-sided. t(4) = 1.011, *P=0.3691.* DMSO: 0.5135 ± 0.08208, n=3; M1: 0.3761 ± 0.1083, n=3 biologically independent isolations), GAPDH was used as a loading control (n=3). All error bars reflect the Mean ± S.E.M.

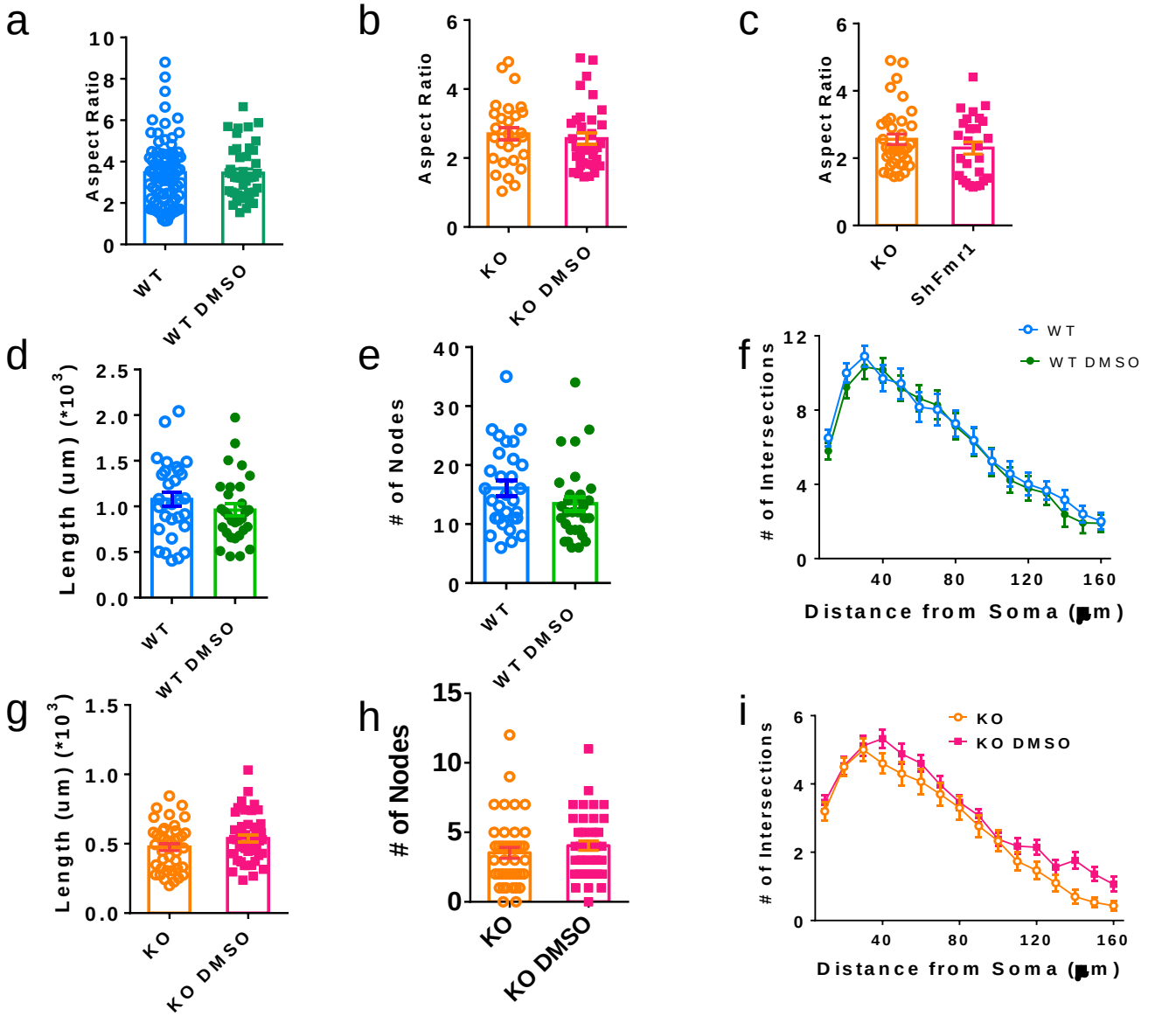

Supplementary Figure 14: Treatment with DMSO did not affect dendritic morphology. a-c, Mitochondrial aspect ratio: a, WT DMSO compared with WT (Student's t-test, two-sided. t(123) = 0.07338, *P* = 0.9416. WT = 3.470 ± 0.1767, n = 81; WT DMSO = 3.449 ± 0.1928, n = 44 cells from 3 biologically independent isolations). **b,** KO DMSO compared with KO (Student's t-test, two-sided. t(62) = 0.5926, *P* = 0.5556. KO = 2.702 ± 0.1834, n = 28; KO DMSO = 2.561 ± 0.1544, n = 36 cells from 3 biologically independent isolations). **c,** KO DMSO compared with WT transfected with shFmr1 (Student's t-test, two-sided. t(61) = 1.094, *P* = 0.2784. KO = 2.561 ± 0.1544, n = 36; *shFmr1* = 2.302 ± 0.1799, n = 27 cells from 3 biologically independent isolations). **d-i,** Dendritic branching analysis: **d,** Length, WT DMSO compared with WT (Student's t-test, two-sided. t(58) = 1.139, *P* = 0.2592. WT = 1.076 ± 0.07701, n = 30; WT DMSO = 0.9594 ± 0.06673, n = 30 cells from 3 biologically independent isolations). **e,** Nodes, WT DMSO compared with WT (Student's t-test, two-sided. t(58) = 1.499, *P* = 0.1393. WT = 16.07 ± 1.272, n = 30; WT DMSO = 13.47 ± 1.179, n = 30 cells from 3 biologically independent isolations). **f, I**ntersections, WT DMSO compared with WT (Student's t-test, two-sided. t(123) = 0.07338, *P* = 0.9416. WT, n = 30; WT DMSO, n = 30 cells from 3 biologically independent isolations). **g,** Length, KO DMSO compared with KO (Student's t-test, two-sided. t(81) = 1.616, *P* = 0.1100. KO = 0.4768 ± 0.02672, n = 40; KO DMSO = 0.5379 ± 0.02668, n = 43 cells from 3 biologically independent isolations). **h,** Nodes, KO DMSO compared with KO (Student's t-test, two-sided. t(81) = 1.010, *P* = 0.3157. KO = 3.525 ± 0.3971, n = 40; KO DMSO = 4.047 ± 0.3344, n = 43 cells from 3 biologically independent isolations). **i, I**ntersections, KO DMSO compared with KO (Student's t-test, two-sided. t(123) = 0.07338,. *P* = 0.9416. KO, n = 40; KO DMSO, n = 43 cells from 3 biologically independent isolations). All error bars reflect the Mean ± S.E.M.

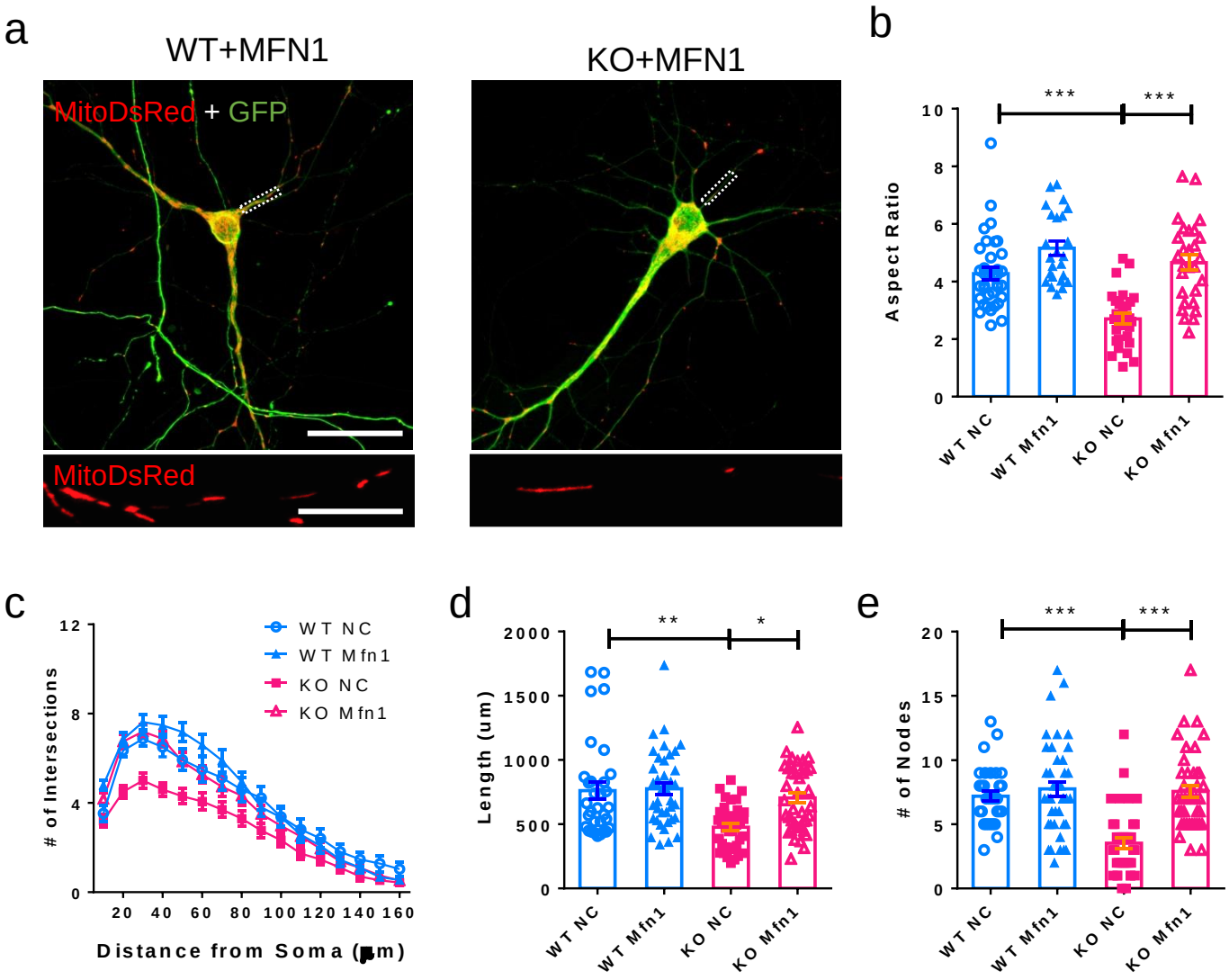

Supplementary Figure 15: Restoration of MFN1 attenuated dendritic maturation deficits in FMRP-deficient developing neurons.

a, Sample confocal images (from 3 independently repeated isolations with similar results) of mitochondria in the *Fmr1* KO and WT hippocampal neurons transfected with Mfn1 or NC. Enlarged view of the boxed area is shown at the bottom of each image.. Scale bars, 20 μm. **b,** Quantification of mitochondrial aspect ratio (Two-way ANOVA with Bonferroni post hoc test, two-sided: treatment × genotype: F (1, 108) = 6.277. $P = 0.0137$. WT:NC vs. KO:NC, $P < 0.0001$; KO:NC vs. KO:Mfn1, $P < 0.0001$. WT:NC = 4.271 ± 0.2085, n = 36; KO:NC = 2.702 ± 0.1834, n = 28; WT:Mfn1 = 5.044 ± 0.2653, n = 20; KO:Mfn1 = 4.655 ± 0.2666, n = 28 cells from 3 independent isolations). **c,** Sholl analysis of dendritic complexity (Multi-ANOVA, KO NC vs. KO Mfn1: F(1,69) = 13.678, $P < 0.0001$. WT:NC, n = 32; KO:NC, n = 40; WT:Mfn1, n = 40; KO:Mfn1, n = 40 cells from 3 independent isolations). **d,** Quantification of dendritic length (Two-way ANOVA with Bonferroni post hoc test, two-sided: treatment × genotype: F (1, 148) = 5.613. $P = 0.0191$. WT:NC, 761.3 ± 66.84, n = 32; KO:NC, 476.8 ± 26.72, n = 40; WT:Mfn1, 775.6 ± 45.58, n = 40; KO:Mfn1, 476.8 ± 26.72, n = 40 cells from 3 independent isolations). **e,** Quantification of dendritic nodes (Two-way ANOVA with Bonferroni post hoc test, two-sided: treatment × genotype: F (1, 148) = 13.09. $P < 0.001$. WT:NC, 7.188 ± 0.3951, n = 32; KO:NC, 3.525 ± 0.3971, n = 40; WT:Mfn1, 7.750 ± 0.5771, n = 40; KO:Mfn1, 7.550 ± 0.4776, n = 40 cells from 3 independent isolations). *P < 0.05, **P < 0.01, ***P < 0.001. All error bars reflect the Mean ± S.E.M.

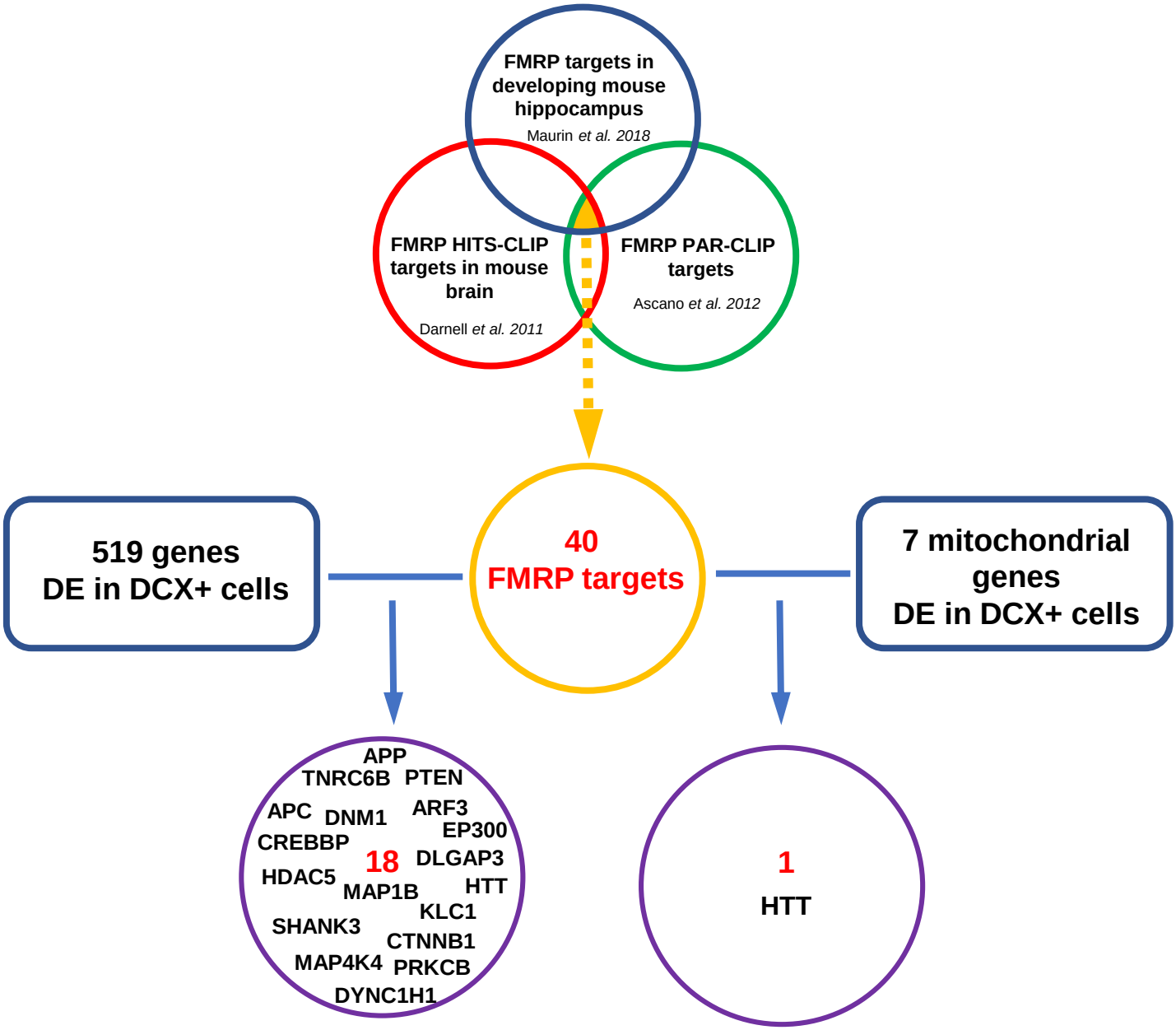

Supplementary Figure 16: Workflow for selecting FMRP targets that may regulate mitochondria in DCX+ immature neurons

a

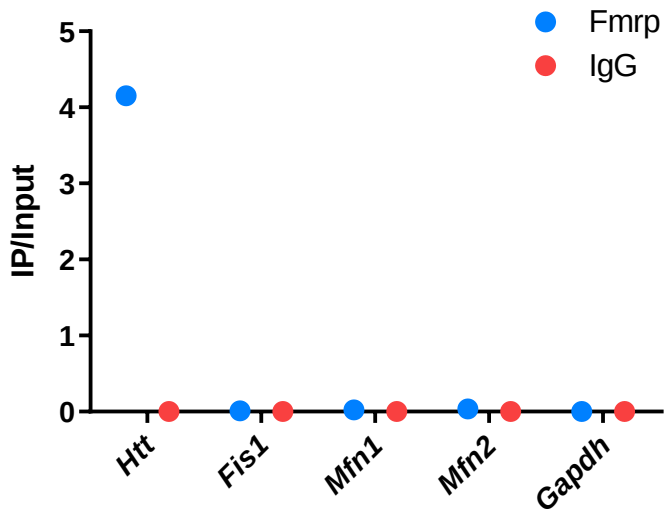

b

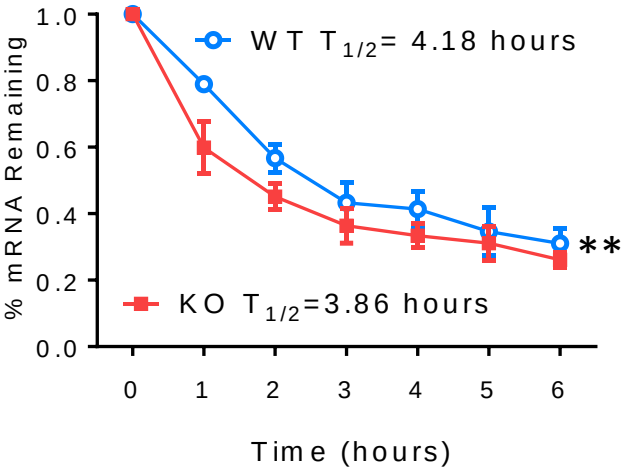

Supplementary Figure 17: FMRP regulates *Htt* mRNA

a. FMRP RNA-IP followed by quantitative real-time PCR analyses for *Htt, Fis1, Mfn1, Mfn2* and *Gapdh* (as negative control) mRNAs in DG of 3-week old mice (average of technical duplicates from one animal are shown). **b.** Assessment of *Htt* mRNA stability in *Fmr1* WT and KO DIV7 primary hippocampal neurons treated with actinomycin D to inhibit transcription. The amount of *Htt* mRNA was quantified using real-time PCR. Half-life of decay was calculated after transforming data to ln. Two-way ANOVA: Genotype F (1, 21) = 10.93 **P = 0.0034. WT: n=3, KO: n=3 biologically independent isolations. **P < 0.01, ***P < 0.001. All error bars reflect the Mean ± S.E.M.

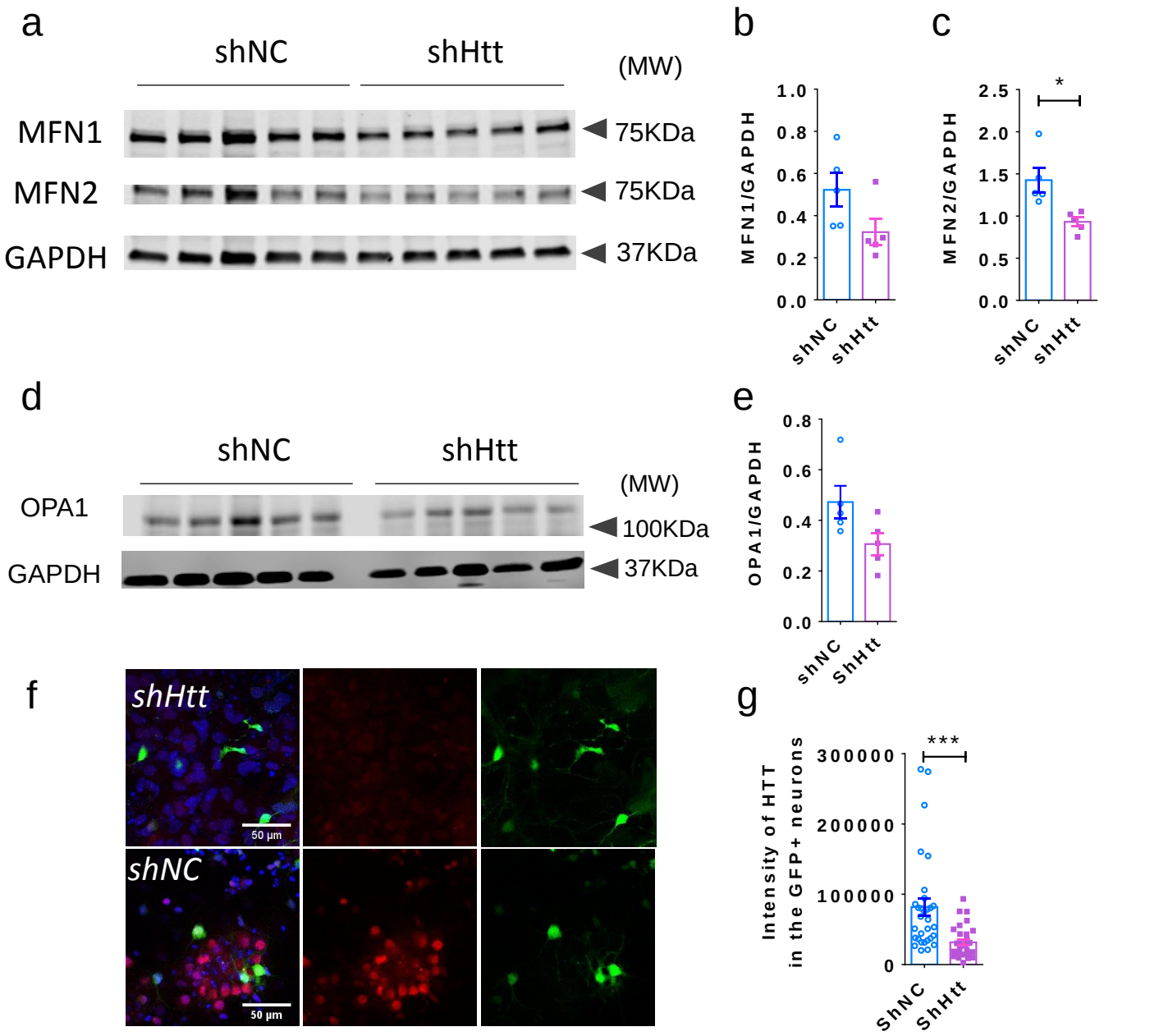

Supplementary Figure 18. Mitofusin and fission protein levels in lentivirus-*shHtt* infected primary neurons.

a-e Western blot analyses of mitochondrial fusion and fission proteins in WT primary cells treated with shNC or shHtt. Representative cropped western blot images (see Supplementary Figure 25 for full images of western blots) **(a, d)** and quantitative analysis of MFN1 (**b,** Student's t-test, two-sided. t(8) = 1.983, *P*=0.0827. shNC = 0.5226 ± 0.08057, n = 5; shHtt = 0.3217 ± 0.06140, n = 5 biologically independent isolations), MFN2 (**c,** Student's t-test, two-sided. t(8) = 3.210, *P*=0.0124. shNC = 1.426 ± 0.1444, n = 5; shHtt = 0.9307 ± 0.05432, n = 5 biologically independent isolations), OPA1 (**e,** Student's t-test, two-sided. t(8) = 2.150, *P*=0.0638. shNC = 0.4725 ± 0.06411, n = 5; shHtt = 0.3064 ± 0.04316, n = 5 biologically independent isolations). GAPDH was used as a loading control. **f-g,** Signal intensity measurement of HTT in WT primary neurons infected with Lv-shNC and Lv-shHtt. **f,** Representative image of primary cells stained with dapi (blue), anti-HTT (red),and GFP (green) . 3 independently repeated experiments with similar results. **g,** Quantitative analysis of HTT signal intensity in GFP positive cells intensity (Student's t-test, two-sided. t(59) = 3.808. *P* < 0.0001. shNC = 81897 ± 12348, n = 31; shHtt = 31626 ± 4145, n = 30 cells from 3 biologically independent isolations). **P* < 0.05, ****P* < 0.001. All error bars reflect the Mean ± S.E.M.

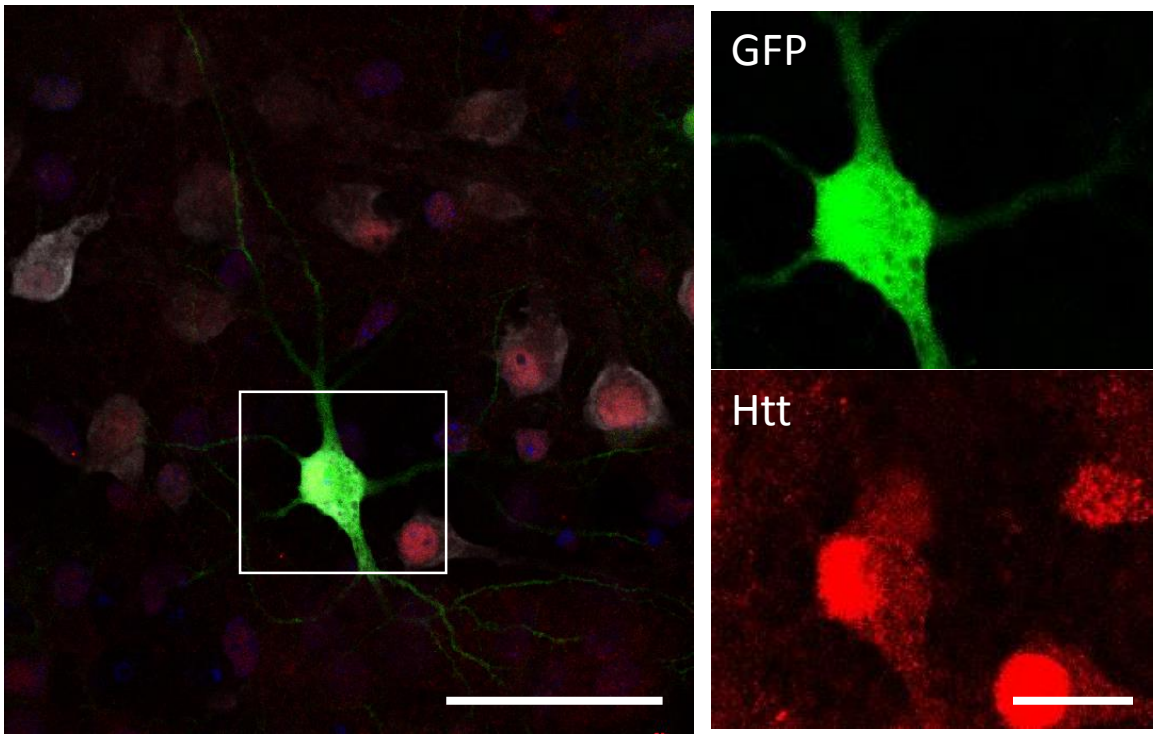

Supplementary figure 19: HTT expression in neurons with CRISPR/dCas9-tageted activation.
Representative image (from 3 independently repeated experiments with similar results) of primary hippocampal neurons with CRISPR/dCas9-tageted *Htt* gene activation. Neurons were stained with antibodies against HTT (red) and GFP (green). Scale bar, 50um.

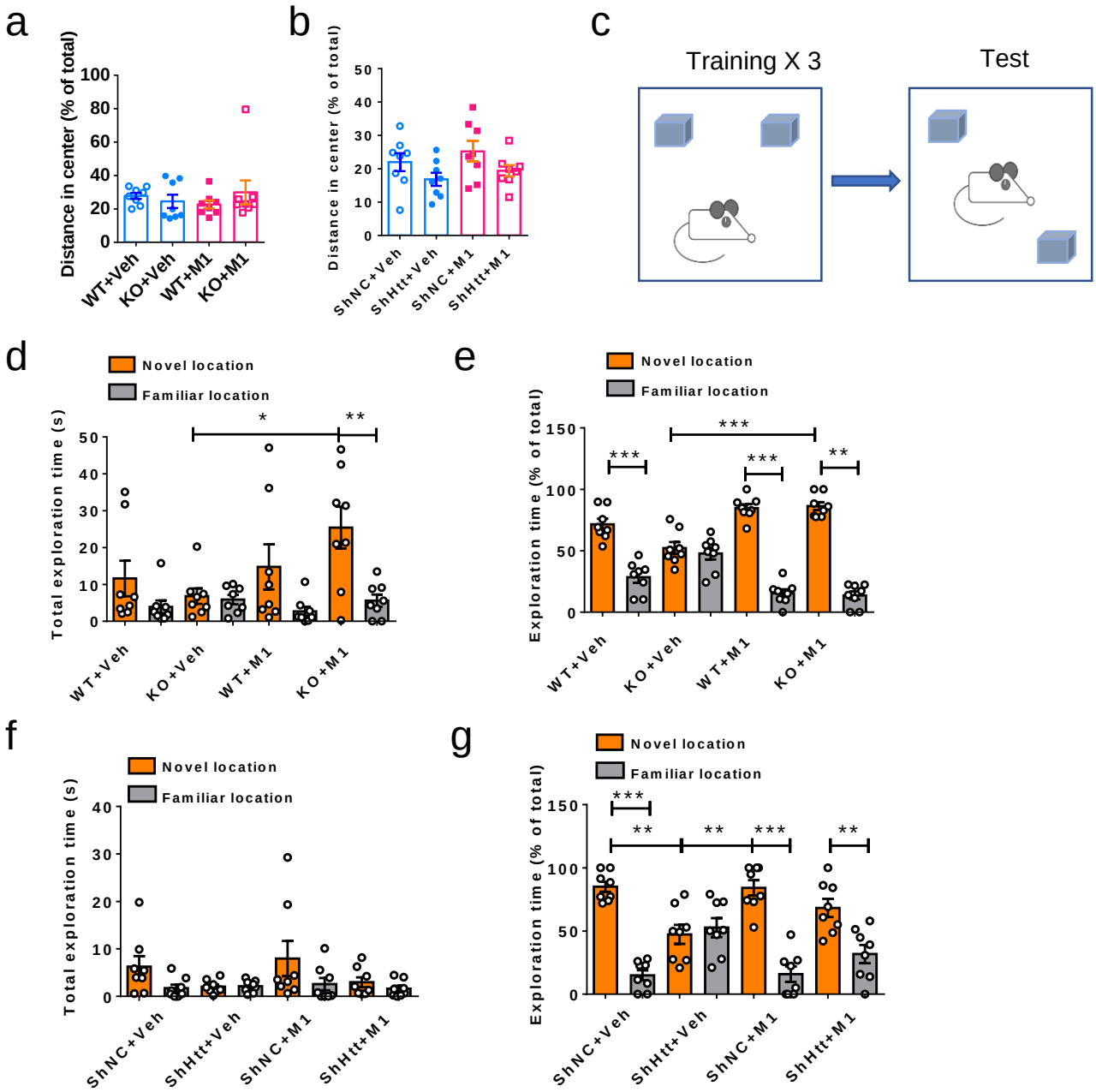

Supplementary figure 20 : Open field activity and Novel location test of Fmr1 KO mice and WT mice with lentiviral injection followed by M1 treatment

a,b Percentage of distance Fmr1 KO/WT (**a**) and virus-injected mice (**b**) travelled in the center field compared to whole filed (n = 8 mice per group). **c** Experimental scheme for assessing spatial memory. **d, e** WT and *Fmr1* KO mice with M1 treatment (n = 8 mice per group). **f, g** WT mice with lentiviral injection followed by M1 treatment (n = 8 mice per group). Total exploration time (**d,** Novel location: KO+Veh vs. KO+M1: $P = 0.0108$. KO+M1 Novel vs. familiar location: $P = 0.0053$. **f**) and percentage exploration time (**e,** WT+Veh: Novel vs. familiar location: $P < 0.0001$; WT+M1: Novel vs. familiar location: $P < 0.0001$; KO+M1: Novel vs. familiar location: $P < 0.0001$; Novel location: KO+Veh vs. KO+M1: $P < 0.0001$. **g,** ShNC+Veh: Novel vs. familiar location: $P < 0.0001$; ShNC+M1: Novel vs. familiar location: $P < 0.0001$; ShHtt+M1: Novel vs. familiar location: $P = 0.009$. Novel location: ShNC+Veh vs. ShHtt+Veh: $P = 0.0062$; ShNC+M1 vs. ShHtt+Veh: $P = 0.0082$) of novel location test are shown. Two-way ANOVA with two-sided Bonferroni post hoc analysis for multiple comparisons. *$P < 0.05$, **$P < 0.01$, ***$P < 0.001$. Data are presented as mean ± SEM.

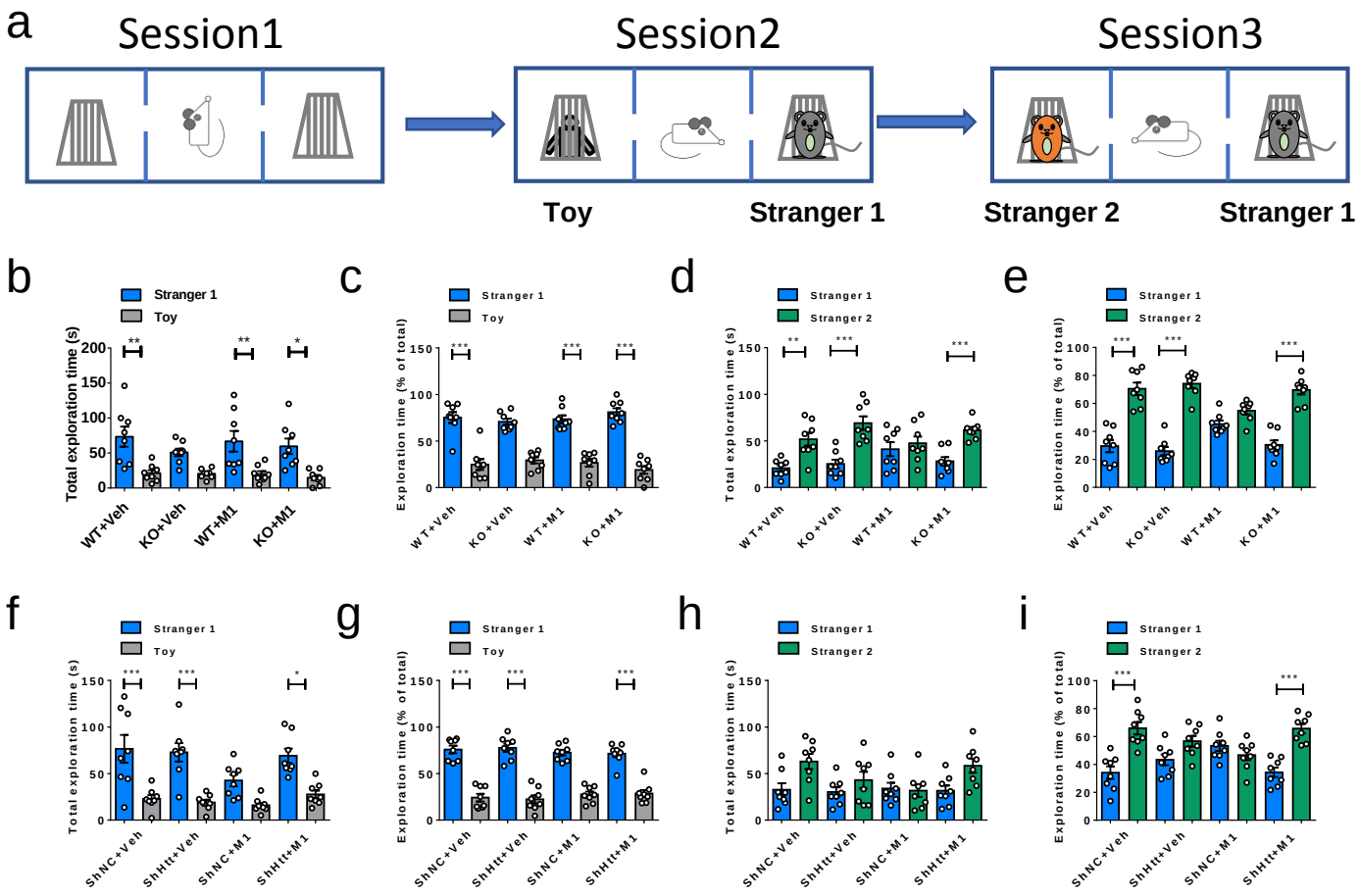

Supplementary figure 21: Social interaction test in Fmr1 KO mice and WT mice with lentiviral injection followed by M1 treatment

a Experimental scheme for assessing social learning. **b-e** WT and *Fmr1* KO mice with M1 treatment. **f-i** WT mice with lentiviral injection followed by M1 treatment (n = 8 mice per group). Total exploration time of first trial (**b,** Stranger 1 vs. Toy, WT+Veh: $P = 0.0014$; WT+M1: $P = 0.0062$; KO+M1: $P = 0.0103$. **f,** Stranger 1 vs. Toy, ShNC+Veh: $P = 0.0004$; ShHtt+Veh: $P = 0.0004$; ShHtt+M1: $P = 0.0146$), total exploration time of second trial (**d,** Stranger 1 vs. Stranger 2, WT+Veh: $P = 0.0024$; WT+M1: $P < 0.0001$; KO+M1: $P = 0.0009$. **h**), percentage exploration time of first trial (**c,** Stranger 1 vs. Toy, WT+Veh: $P < 0.0001$; WT+M1: $P < 0.0001$; KO+M1: $P < 0.0001$. **g,** Stranger 1 vs. Toy, ShNC+Veh: $P < 0.0001$; ShHtt+Veh: $P < 0.0001$; ShHtt+M1: $P < 0.0001$), and percentage exploration time of second trial (**e,** Stranger 1 vs. Stranger 2, WT+Veh: $P < 0.0001$; WT+M1: $P < 0.0001$; KO+M1: $P < 0.0001$. **i,** Stranger 1 vs. Stranger 2, ShNC+Veh: $P < 0.0001$; ShHtt+M1: $P < 0.0001$) for the social interaction test are shown. Two-way ANOVA with two-sided Bonferroni post hoc analysis for multiple comparisons. *$P < 0.05$, **$P < 0.01$, ***$P < 0.001$. Data are presented as mean ± SEM.

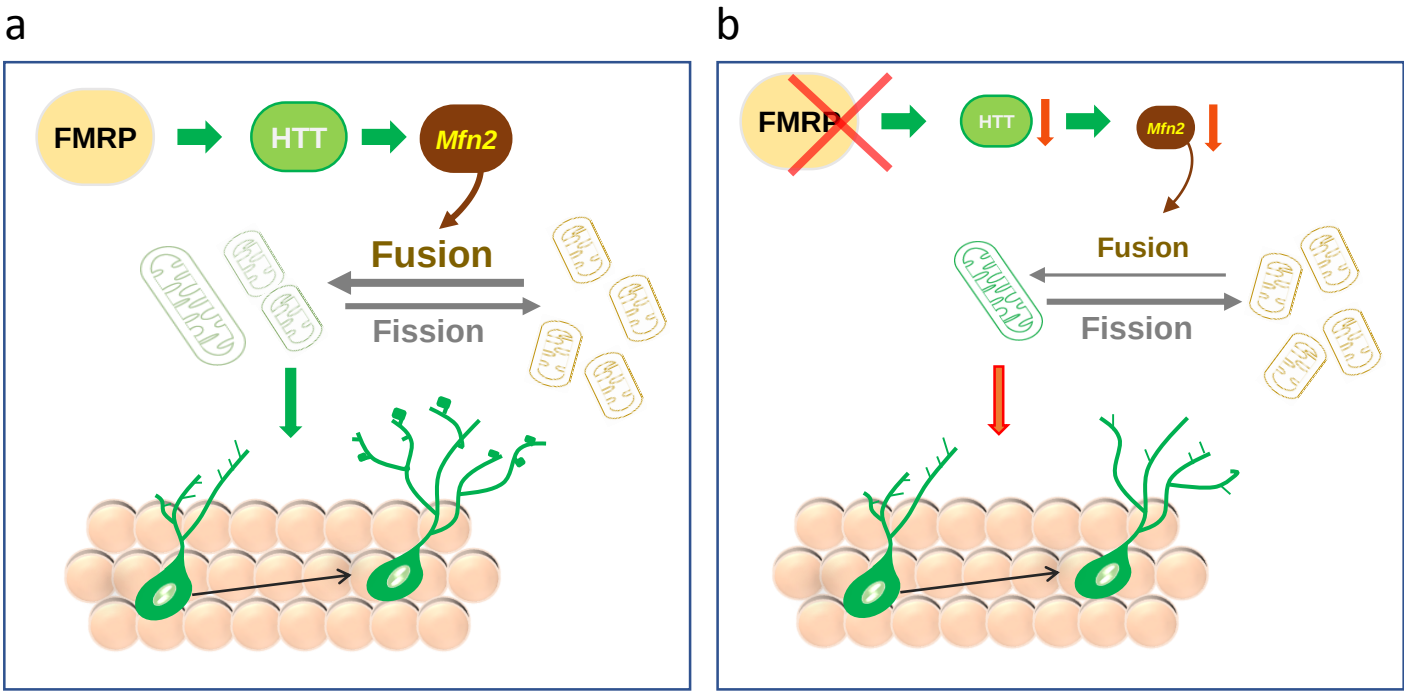

Supplementary Figure 22. Models for FMRP regulation of mitochondrial fusion and neuronal maturation.
a, Physiological regulation of FMRP on HTT and mitochondrial fusion in neuronal maturation. **b,** Deficits of HTT, mitochondrial fusion and neuronal maturation in FXS mouse model.

Supplementary figure 12a

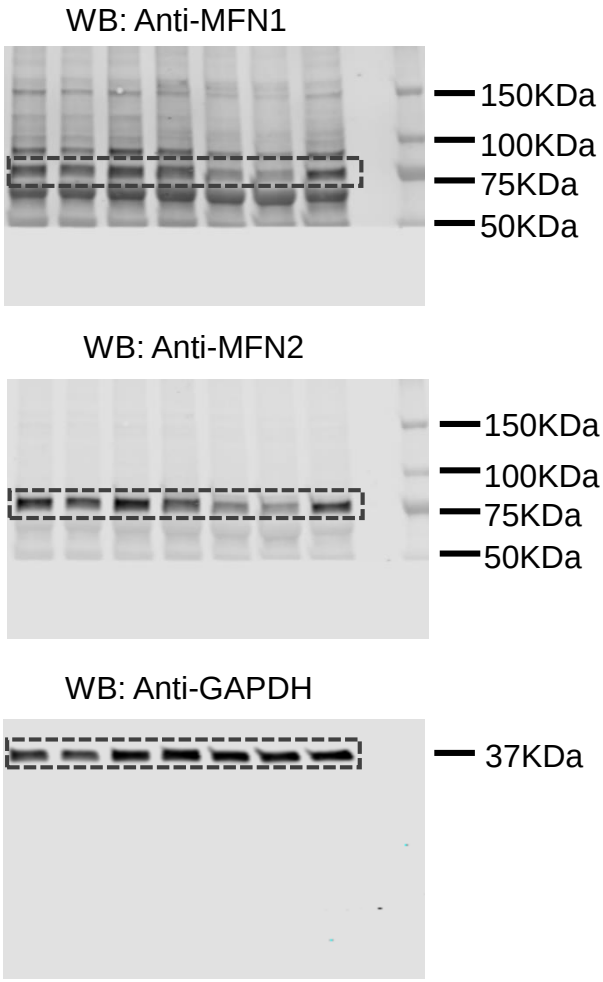

Supplementary figure 12d

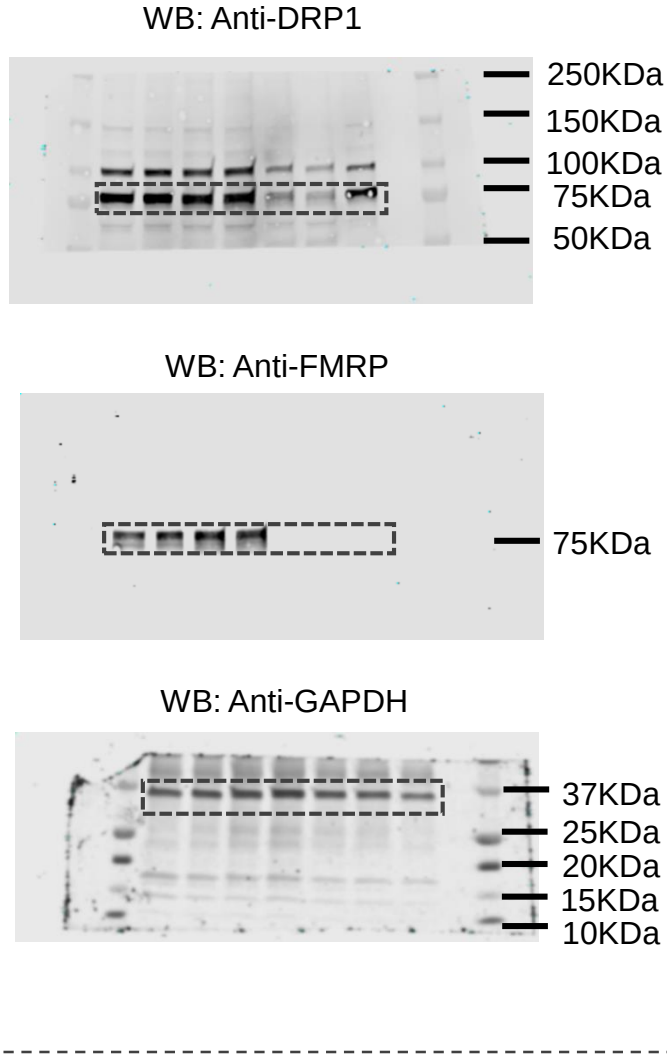

Supplementary figure 12g

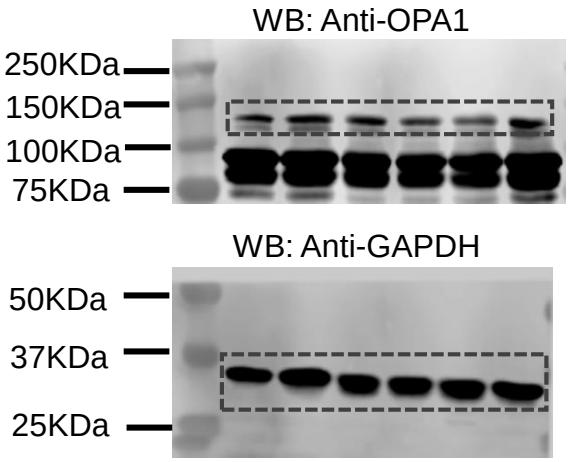

Supplementary Figure 23. Full images of western blots used for supplementary figure 12

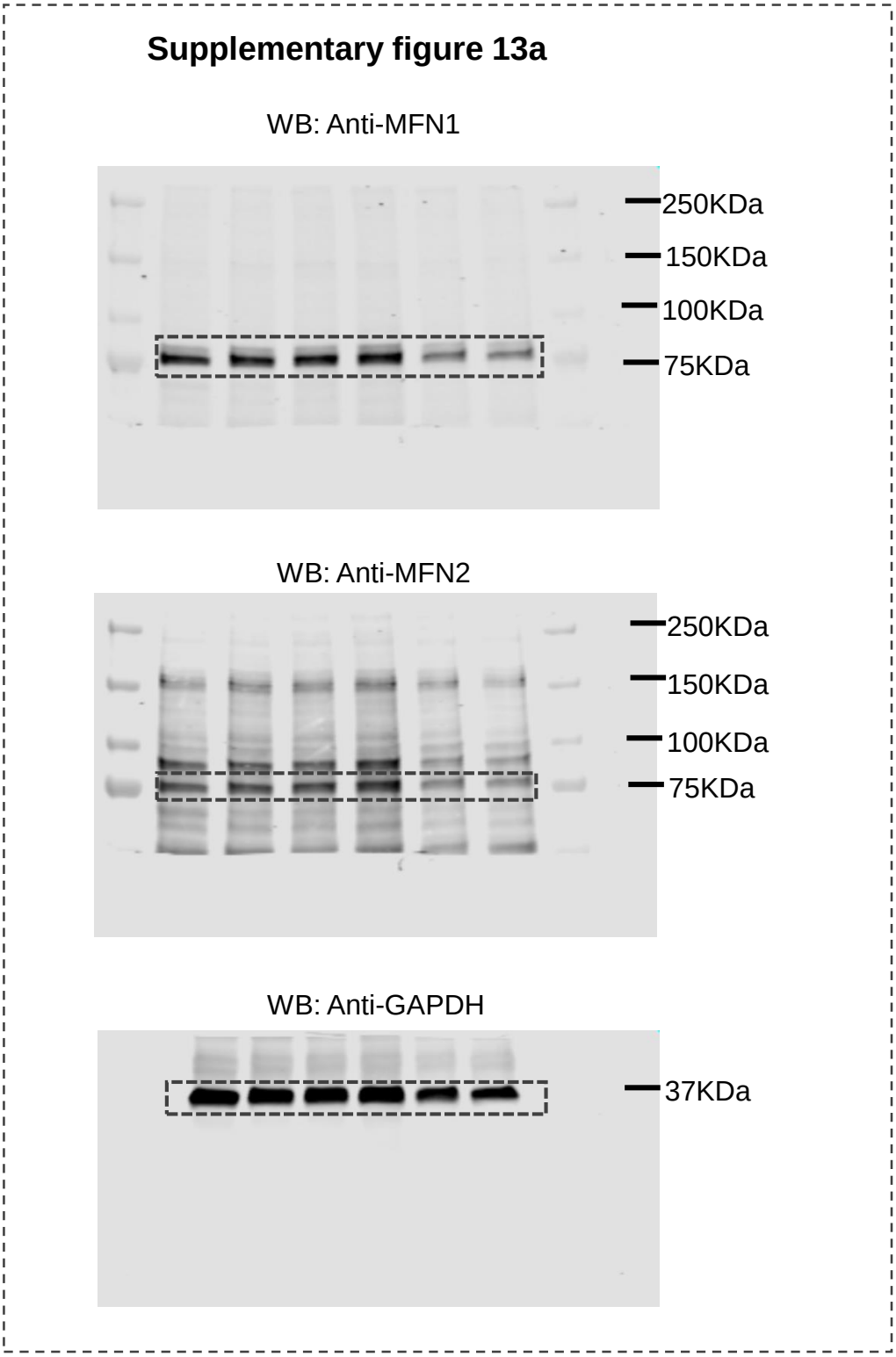

Supplementary Figure 24. Full images of western blots used for supplementary figure 13

Supplementary figure 18a

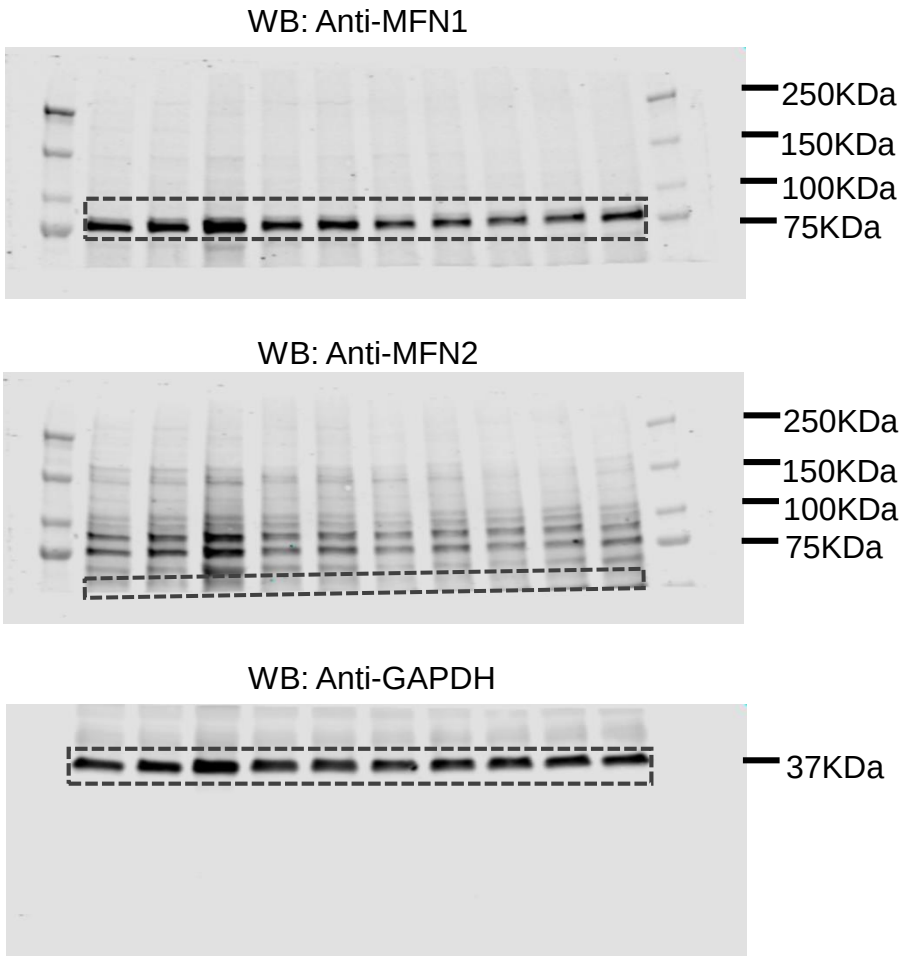

Supplementary figure 18d

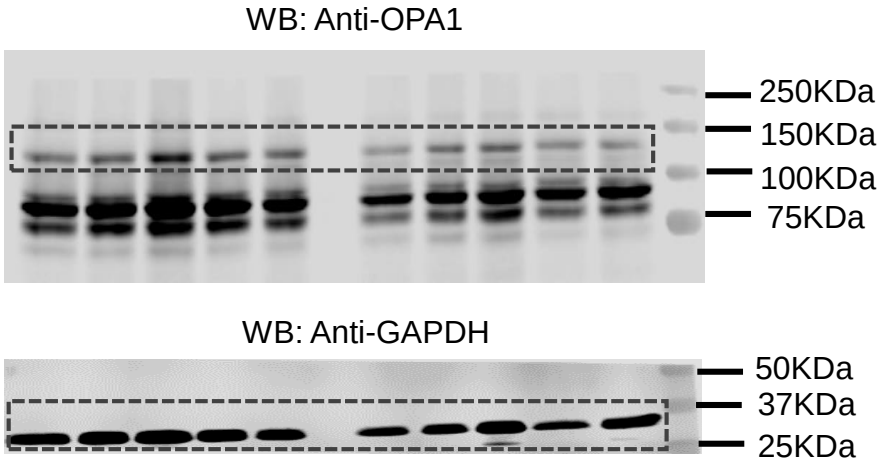

Supplementary Figure 25. Full images of western blots used for supplementary figure 18